Oblique aggradation

A novel explanation for sinuosity of low-energy streams in peat-filled valley systems

Candel, Jasper H J; Makaske, Bart; Storms, Joep E A; Wallinga, Jakob

DOI
10.1002/esp.4100

Publication date
2017

Document Version
Final published version

Published in
Earth Surface Processes and Landforms

Citation (APA)
Candel, J. H. J., Makaske, B., Storms, J. E. A., & Wallinga, J. (2017). Oblique aggradation: A novel explanation for sinuosity of low-energy streams in peat-filled valley systems. *Earth Surface Processes and Landforms*, *42*(15), 2679-2696. https://doi.org/10.1002/esp.4100

EARTH SURFACE PROCESSES AND LANDFORMS
Earth Surf. Process. Landforms (2017)

Published online in Wiley Online Library
(wileyonlinelibrary.com) DOI: 10.1002/esp.4100

Oblique aggradation: a novel explanation for sinuosity of low-energy streams in peat-filled valley systems

Jasper H.J. Candel,[1]* Bart Makaske,[1] Joep E.A. Storms[2] and Jakob Wallinga[1]
[1] Soil Geography and Landscape group, Wageningen University, P.O. Box 47, 6700AA Wageningen, The Netherlands
[2] Faculty of Civil Engineering and Geosciences, Delft University of Technology, P.O. Box 5048, 2628CN Delft, The Netherlands

Received 1 July 2016; Revised 2 December 2016; Accepted 7 December 2016

*Correspondence to: Jasper Candel, Wageningen University, Soil Geography and Landscape group, P.O. Box 47, 6700AA Wageningen, The Netherlands.
E-mail: jasper.candel@wur.nl

ESPL
Earth Surface Processes and Landforms

ABSTRACT: Low-energy streams in peatlands often have a high sinuosity. However, it is unknown how this sinuous planform formed, since lateral migration of the channel is hindered by relatively erosion-resistant banks. We present a conceptual model of Holocene morphodynamic evolution of a stream in a peat-filled valley, based on a palaeohydrological reconstruction. Coring, ground-penetrating radar (GPR) data, and ^{14}C and OSL dating were used for the reconstruction. We found that the stream planform is partly inherited from the Late-Glacial topography, reflecting stream morphology prior to peat growth in the valley. Most importantly, we show that aggrading streams in a peat-filled valley combine vertical aggradation with lateral displacement caused by attraction to the sandy valley sides, which are more erodible than the co-evally aggrading valley-fill. Owing to this oblique aggradation in combination with floodplain widening, the stream becomes stretched out as channel reaches may alternately aggrade along opposed valley sides, resulting in increased sinuosity over time. Hence, highly sinuous planforms can form in peat-filled valleys without the traditional morphodynamics of alluvial bed lateral migration. Improved understanding of the evolution of streams provides inspiration for stream restoration. Copyright © 2016 John Wiley & Sons, Ltd.

Introduction

Predicting stream morphodynamics is a key aspect in stream restoration projects, in order to prevent flooding or unwanted bank erosion, and to plan and minimize management (Eekhout *et al.*, 2015). Currently, a knowledge gap exists between stream restoration demands and current understanding on the morphodynamic functioning of low-energy streams (Wohl *et al.*, 2005; Walter and Merritts, 2008; Lespez *et al.*, 2015). In many stream restoration projects in lowlands, single-thread, sinuous streams are often seen as 'natural' and used as a reference. Sometimes this reference is derived from historical maps (Kondolf, 2006). However, it is often unknown when the sinuous planform formed and whether streams laterally migrated in the past. Some studies found evidence that the sinuous planform of low-energy streams may be the consequence of historical land-use changes that started around the Bronze Age (Broothaerts *et al.*, 2014; Lespez *et al.*, 2015) or later (Kondolf *et al.*, 2002), or may be the result of historical water engineering (e.g. for watermills) (Walter and Merritts, 2008). Since morphodynamic processes in low-energy streams are slow, these processes should be studied on a longer time scale using palaeohydrological approaches in order to constrain future morphological stream behaviour (Grabowski *et al.*, 2014). Palaeohydrology is defined as 'the study of fluvial processes and their hydrological implications before the onset of instrumental records' (Thorndycraft, 2013), and is becoming a more important discipline needed to understand and manage rivers and streams (Sear and Arnell, 2006). The discipline has made considerable progress in developing relevant knowledge and tools for water managers (Brierley and Fryirs, 2000; Kondolf *et al.*, 2003b).

There are several types and settings of low-energy streams (Kondolf *et al.*, 2003a). Here we use a recent classification scheme for European streams by Gurnell *et al.* (2014) that builds on the classification scheme of Nanson and Croke (1992). They define low-energy streams as those having a stream power of less than 10 W m^{-2}. Low-energy streams can be divided into anabranching streams and single-thread streams, and can further be subdivided into streams with inorganic floodplains (Brown and Keough, 1992; Notebaert and Verstraeten, 2010; Eekhout *et al.*, 2015) and organic floodplains, i.e. peatlands (Prosser *et al.*, 1994; Gradziński *et al.*, 2003; Watters and Stanley, 2007; Nanson, 2009). Low-energy streams are often classified as non-dynamic, with a stream power too limited to induce morphodynamic processes (Kleinhans *et al.*, 2009; Kleinhans and Van den Berg, 2011; Eekhout *et al.*, 2014), especially in peatlands, since peatbanks are relatively erosion-resistant (Micheli and Kirchner, 2002a, b; Gradziński *et al.*, 2003; Nanson, 2010; Stenberg *et al.*, 2015). At the same time,

peatland streams often have a high sinuosity and tight meander bends (Jurmu and Andrle, 1997), but the morphodynamics of such systems has received little attention to date.

In general, hydraulic processes are responsible for the in-channel morphology (Nanson, 2010; Nanson *et al.*, 2010), in some cases in combination with biological processes by plants and their non-degrading remnants which may build and stabilize the channel banks (Gradziński *et al.*, 2003; Watters and Stanley, 2007; Gurnell, 2014). Although both processes also act in peatland streams, their relative importance will be different. Traditionally deployed fluid mechanics and empirical geomorphic rules of self-adjusting channels in clastic alluvium seem invalid and should not be applied in peatland streams (Jurmu, 2002; Nanson, 2009, 2010; Nanson *et al.*, 2010). Even though sinuous channels are often found in peatlands, it is unknown how and why the sinuous planform evolved and whether the sinuosity is a result of lateral migration of channels (Gradziński *et al.*, 2003; Nanson and Cohen, 2014). Nanson and Cohen (2014) argue that the steep, stable peat-banks result in high flow-efficient channels. They also argue that the tight meander bends in these sinuous channels are therefore formed to consume the surplus stream power by the creation of secondary currents and turbulence, hence peatland systems attain equilibrium. However, this process still does not explain how, when, and at what rate these bends were formed.

Brown and Keough (1992) and Brown *et al.* (1994) showed that the sinuous planform of low-energy streams in the United Kingdom was inherited from former river styles. They found evidence that the pattern of stream channels changed during the Holocene from braiding rivers into anastomosing rivers, and later into single-thread, laterally stable channels ('stable bed aggrading banks' model). Similarly, such a pattern shift might explain sinuous yet laterally stable channels in peatlands, where the stream planform is inherited from the period prior to peat growth. In addition, it is debated whether natural low-energy systems in peatlands always have had a channel, or that drainage may also have been dispersed in a wetland system. The latter seems to have been the case during the Middle Holocene in some lowland valleys (Nanson, 2009; Broothaerts *et al.*, 2014; Lespez *et al.*, 2015), although it is not clear whether that was a common or an exceptional phenomenon.

The aim of this research is to identify the mechanisms that lead to the formation of highly sinuous planforms in low-energy streams in a peat-filled valley. Our study involves a detailed palaeohydrological reconstruction of the morphodynamic evolution of a peatland stream during the Holocene. We present a new conceptual model for stream planform evolution in this setting, and discuss the implications for streams in similar systems and for future management of these stream types.

Study Area

A study area was chosen where peat growth occurred during the entire Holocene, to cover a long time period with conditions similar to the present. In addition, this area should have a stream that has never been channelized (and also not restored) to relate the present stream morphology to the past morphodynamic functioning. The Drentsche Aa in the north-eastern Netherlands (Figure 1) fitted these criteria.

The Drentsche Aa is one of the few streams in The Netherlands that has never been channelized and still has a sinuous planform for almost its entire length (De Gans, 1981; Spek *et al.*, 2015). Kuenen (1944) highlighted that morphodynamic processes of meandering are lacking in the nevertheless sinuous Drentsche Aa, a finding recently corroborated by a study of historic maps from 1650 to 1900 AD. The Drentsche Aa catchment (300 km^2, Figure 1) is located within subglacially deformed till ridges of the Drenthe till plateau formed 150 000 to 160 000 years ago (Van den Berg and Beets, 1987; Busschers *et al.*, 2008). The formation of the valleys was the result of fast surface runoff of snow meltwater under permafrost conditions during the Weichselian (De Gans, 1981). Coversands were deposited over a large part of the area during this period, reaching thicknesses of 0.5 to 2 m. From the late Weichselian and during the Holocene, the valleys filled with peat, with thicknesses locally reaching up to 7 m (Makaske *et al.*, 2015). Nowadays, the Drentsche Aa is a low-energy stream with a mean annual discharge of 1.8 $m^3 s^{-1}$, a stream power of 0.5 $W m^{-2}$, and the floodplain elevation varies from 16 m + NAP (Dutch Ordnance Datum, ≈ sea level) to 0.7 m + NAP. Most of the catchment area is a national park since 1965, a Unesco Global Geopark since 2015, and functions as a nature conservation reserve with forest and meadows. The land use around the national park is forest and agriculture (cattle and arable farming). Groundwater use for drinking water purposes has been limited since 1989, to prevent additional peat oxidation in the valleys (Meijles, 2015).

Six locations were chosen along the Drentsche Aa for our study (Figure 1). These locations were selected based on equal coverage of the catchment, minimum signs of human disturbance and covering both straight reaches and bends. Three of these sites were part of a previous investigation providing dating and coring data for the locations Loon, Kappersbult and Amen (Makaske *et al.*, 2015). Additional locations were at Schipborg, and two locations at Gasteren (Gasteren1 and Gasteren2). The Gasteren sections are on a tributary of the Drentsche Aa (Figure 1). Figure 2 shows the digital elevation models (DEM, Actueel Hoogtebestand Nederland, 0.5 × 0.5 m) (Van Heerd and Van't Zand, 1999) for all locations. The Drentsche Aa has a width of approximately 3 m at the most upstream location in Amen, in comparison with a width of approximately 15 m at Kappersbult.

Makaske *et al.* (2015) studied the peat growth rate in the Drentsche Aa valley by radiocarbon (^{14}C) dating of *in situ* peat. All their samples were taken on the sandy Pleistocene valley side to minimize the effects of peat compaction on the reconstruction of past water table heights. The ^{14}C data and the absence of layers with strongly degraded peat indicate continuous peat formation, and thus groundwater-level rise, since the Late Glacial until the Middle Ages (Makaske *et al.*, 2015).

Methodology

Lithological description

Six transects were cored with a gouge auger (Ø: 3 cm). The transects were planned using the DEM, and were placed perpendicular to the stream. The transects were located such that the entire floodplain was included. The coring depth varied depending on the depth of the underlying Pleistocene deposits, but did not exceed 8 m. Coring spacing was 5 to 10 m near the current stream, to ensure that all potential channel deposits were sampled, taking into consideration the dimensions of the palaeochannels. The surface elevation of each borehole was measured with a Global Navigation Satellite System (GNSS) device, with a vertical accuracy of approximately 1 to 2 cm. Additional coring data from 2003, 2009 and 2010 was available at Loon, Kappersbult and Amen from Makaske *et al.* (2015). For one site, the original lithological data of one coring was derived from DINOLoket, a national geological borehole database (TNO, 2015), because we could not access the field site. The section Gasteren1 was difficult to auger, owing to the extremely

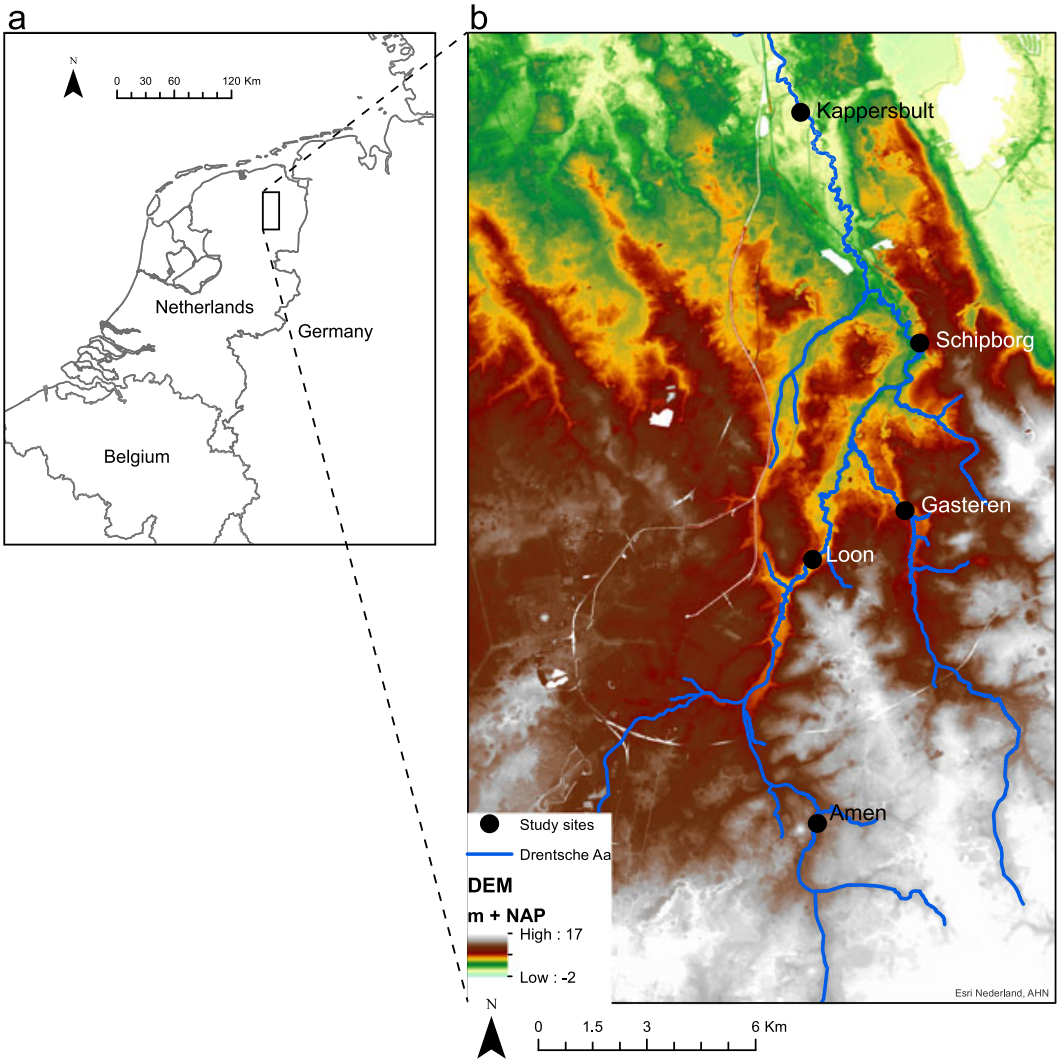

Figure 1. Map of the study area. a) The Drentsche Aa is located in the northeastern Netherlands. b) A DEM (Van Heerd and Van't Zand, 1999) of the Drentsche Aa catchment, including the locations where the stratigraphic cross-sections were made. At Gasteren, two stratigraphic cross-sections were made (Gasteren1 and Gasteren2). [Colour figure can be viewed at wileyonlinelibrary.com]

wet surface conditions. Auger points at this location had to be selected based on the terrain accessibility.

A standard method was used to describe the sediment cores in 10-cm-thick intervals (Berendsen and Stouthamer, 2001). The sediment texture (D_{50}) of non-organic, sandy samples was visually determined in the field by comparison with a sand ruler. Organic samples were visually checked in the field for the presence of sand or loam. At all locations the plant macro-remains were described.

GPR

Ground penetrating radar (GPR) proved to be successful in previous studies in peatlands (Lowry *et al.*, 2009; Proulx-McInnis *et al.*, 2013; Pîrnău *et al.*, 2015). GPR is able to detect layers that have a different bulk density and humification, so it was expected that sand layers within the peat could also be detected (Lapen *et al.*, 1996; Van Overmeeren *et al.*, 1997; Pîrnău *et al.*, 2015). GPR measurements were conducted with a pulseEKKO PRO 200 Hz and 250 Hz with a SmartTow configuration. The GPR was used to cover four of the six cored transects. The other locations were too wet to use GPR (Gasteren1), or contained too much clay resulting in attenuating signals (Kappersbult). The GPR signal reached a depth of approximately 3 m in the peat-filled valley of the Drentsche Aa. The high groundwater levels result in high attenuation of radar signals and limited penetration depth (Wastiaux *et al.*, 2000; Neal, 2004). In the Drentsche Aa valley different lithologies are present in the subsurface, affecting the electromagnetic-wave velocity that determines the depth of attenuation. In freshwater peat the wave has a velocity of 0.03 to 0.06 m ns^{-1}, while in saturated sand the wave has a velocity of 0.05 to 0.08 m ns^{-1} (Neal, 2004). The actual velocity was derived from the GPR profiles by using isolated reflector points (Neal, 2004), and was in all profiles between 0.054 and 0.060 m ns^{-1}. Since the GPR is primarily used to determine the shapes and continuity of lithological layers, the GPR profiles were not corrected for the heterogeneous electromagnetic velocity speeds and slight undulations of the surface elevation. The GPR profiles were interpreted based on expert judgement, and provided insight into the approximate depths and geometry of the lithological features for the upper 3 m. This insight helped to infer the lithogenetic cross-sections from the lithological cross-sections which are based on the coring data.

OSL dating

Optically stimulated luminescence (OSL) dating is a powerful tool in dating sediments from a wide range of depositional environments (Wallinga *et al.*, 2007). OSL dating determines the

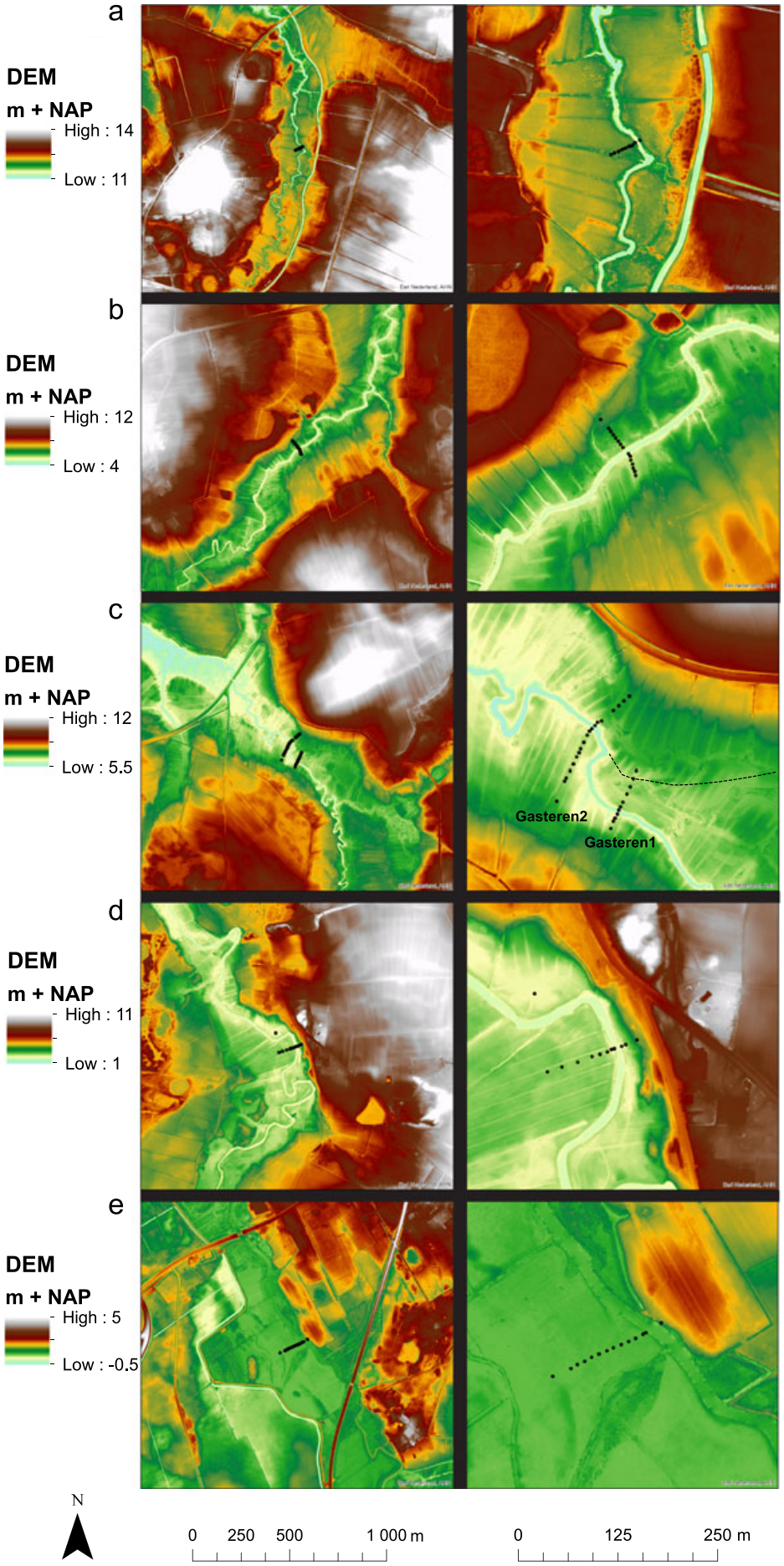

Figure 2. DEM of all study locations, including the coring locations. All locations are shown in two different scales (left & right). a) Amen, b) Loon, c) Gasteren1 (east) & Gasteren2 (west), dashed line indicates the tributary channel found in cross-section Gasteren1, d) Schipborg, and e) Kappersbult. [Colour figure can be viewed at wileyonlinelibrary.com]

last exposure to light of mineral grains (here sand-sized quartz), and thus determines the time of deposition and burial of sediments (Preusser *et al.*, 2008). Four samples for optical stimulated luminescence (OSL) were taken to determine the burial age of sandy deposits within the valley-fill at Schipborg. The OSL samples were taken at different depths in a single borehole at 30 m from the stream using a Van der Staay suction corer (Van de Meene *et al.*, 1979; Wallinga and van der Staay, 1999) for saturated sand, or a modified hand-auger in unsaturated conditions. Both methods use a PVC-tube (Ø 4–4.5 cm) to collect the samples, which ensures that samples are not exposed to light during sampling. The OSL age was determined at the Netherlands Centre for Luminescence dating. In the laboratory, the outer 3 cm of all samples was removed and a sample of 300 to 500 g was left for the analysis and split into two parts under orange/amber safelights. One part was prepared for dose rate analysis and the other part for equivalent dose estimation.

Bulk samples were dried for 24 h at 105°C, weighed, and ashed for 24 h at 500°C; water and organic content was determined during this procedure. The sample was ground and cast in wax to ensure radon retention, and radionuclide concentrations were measured using a broad-energy gamma spectrometer. Dose rates were calculated using the conversion factors of Guérin *et al.* (2011) taking into account contributions from cosmic rays (Prescott and Hutton, 1994), as well as attenuation by water, organics and grain size (Aitken, 1985; Madsen *et al.*, 2005).

Quartz extracts of coarse grains (212–250 μm) were obtained through sieving and treatment with HCl, H_2O_2 and HF. For each sample, small aliquots (2 mm diameter) were prepared on stainless-steel discs sprayed with a thin layer of silicon. Measurements were performed on a Risø TL/OSL DA20 reader (Bøtter-Jensen *et al.*, 2003), using the single-aliquot regenerative dose (SAR) protocol (Wintle and Murray, 2006). A relatively low preheat of 200°C and cutheat of 180°C were used, to prevent thermal transfer effects. Early background subtraction was used to maximize the contribution from the quartz fast-OSL component (Cunningham and Wallinga, 2010). Around 45 aliquots were measured per sample. A bootstrapped version of the Minimum Age Model (Galbraith *et al.*, 1999; Cunningham and Wallinga, 2012) was used to estimate burial doses from scattered equivalent dose distributions, assuming an overdispersion of $20 \pm 5\%$ not related to heterogeneous bleaching (Cunningham *et al.*, 2011). Burial ages were determined by dividing the equivalent dose by the dose rate, taking all uncertainties in both into account. Results are reported with 1-sigma errors.

^{14}C dating

First we briefly describe the methods used by Makaske *et al.* (2015) for collecting and dating peat samples. Their samples were taken at the sand–peat interface with a gouge auger (Ø: 4 cm). In the laboratory, the sample was cut in 1 cm thick slices and sieved with a mesh size of 180 μm. Suitable material was selected by using a microsope and samples were stored in diluted HCl. Terrestrial macro-remains such as leaves and seeds were preferably used for the analysis to prevent an under- or overestimation of the ^{14}C age (Mook and Streurman, 1983; Törnqvist *et al.*, 1992). However, due to the lack of recognizable macro-remains also wood or unrecognizable plant remains were used. From the residue and filtrate the sand content was determined. The sand–peat interface was based on a volumetric sand content lower than 10 to 20%. The macro-remains from the centimeter above this interface were selected for the ^{14}C analysis. In total 15 samples of selected macro-remains were dated at the Accelerator Mass Spectrometry (AMS) facility of the Leibniz Laboratory for Radiometric Dating and Stable Isotope Research. For calibration, the IntCal9 curve was used in the Wincal25 software (Van der Plicht, 2005; Reimer *et al.*, 2009).

One additional sample for ^{14}C analysis was taken in this study from terrestrial macro-remains (alder wood) in the same borehole as the OSL samples, below the sedimentary unit at a depth of 420 cm (Figure 7(a)). The matrix around the alder wood had all the characteristics of the described lithogenetic *in situ* peat unit (see lithogenetic unit description). The ^{14}C age was determined by AMS at the Centre for Isotope Research (Groningen University). For calibration, the IntCal13 curve was used in the OxCal4.2.4 software (Bronk Ramsey, 2009; Reimer *et al.*, 2013).

Inferences on lithogenesis

The cross-section figures are set up with different panels, starting with a geological overview cross-section (after Makaske *et al.*, 2015), followed by a lithological, an interpreted GPR, and a lithogenetic cross-section (Figures 3–8), if all these data were present for the specific location. The lithogenetic cross-sections are constructed based on the combination of all the available information for each section. The first step was to distinguish units based on their lithology and additional characteristics found during the coring, e.g. presence of macro-remains or layering. The second step was combining this information with the extent and shape of each unit, obtained through closely spaced cores and GPR data for the upper 3 m (original GPR profiles in Supporting information). The DEM was also used for the near-surface stratigraphy, since surface elevations can help in identifying morphological features. For example, old channel beds or overbank deposits were easily recognized from the GPR and DEM by their geometry, which in combination with the lithology from the boreholes helped in distinguishing the units in the lithogenetic cross-sections. The last step involved using the OSL and ^{14}C data (Table I and II) to validate the stratigraphical order of the lithogenetic units at Schipborg. ^{14}C ages from the valley fill at the palaeovalley margins provide information on timing and rate of peat development in the valley. However, because of differential compaction related to valley shape and loading effects, isochrones are not expected to be horizontal.

Results

Lithogenetic units

In situ peat contains plant macrofossils, mostly alder and some oak wood, and sedge roots and leafs. Wood pieces can reach thicknesses in boreholes of 0.5 m. The unit does not contain observable clastic sediments. The colour of this lithogenetic unit is dark brown, but turns black when exposed to air. Plant remains are interwoven, resulting in a firm structure. This lithogenetic unit corresponds to the description of *in situ* peat by Bos *et al.* (2012). *In situ* peat is mostly found as the matrix in which other lithogenetic units are present.

Fluvial deposits may consist of peat with clastic sediments, but also clay, silt or sand with an extremely fine to coarse texture (75–600 μm). The unit can show well developed bedding, varying from several centimeters to several decimeters in thickness. Sometimes a thinning upward succession was recognized. The clastics can be poorly sorted. The colour is light to

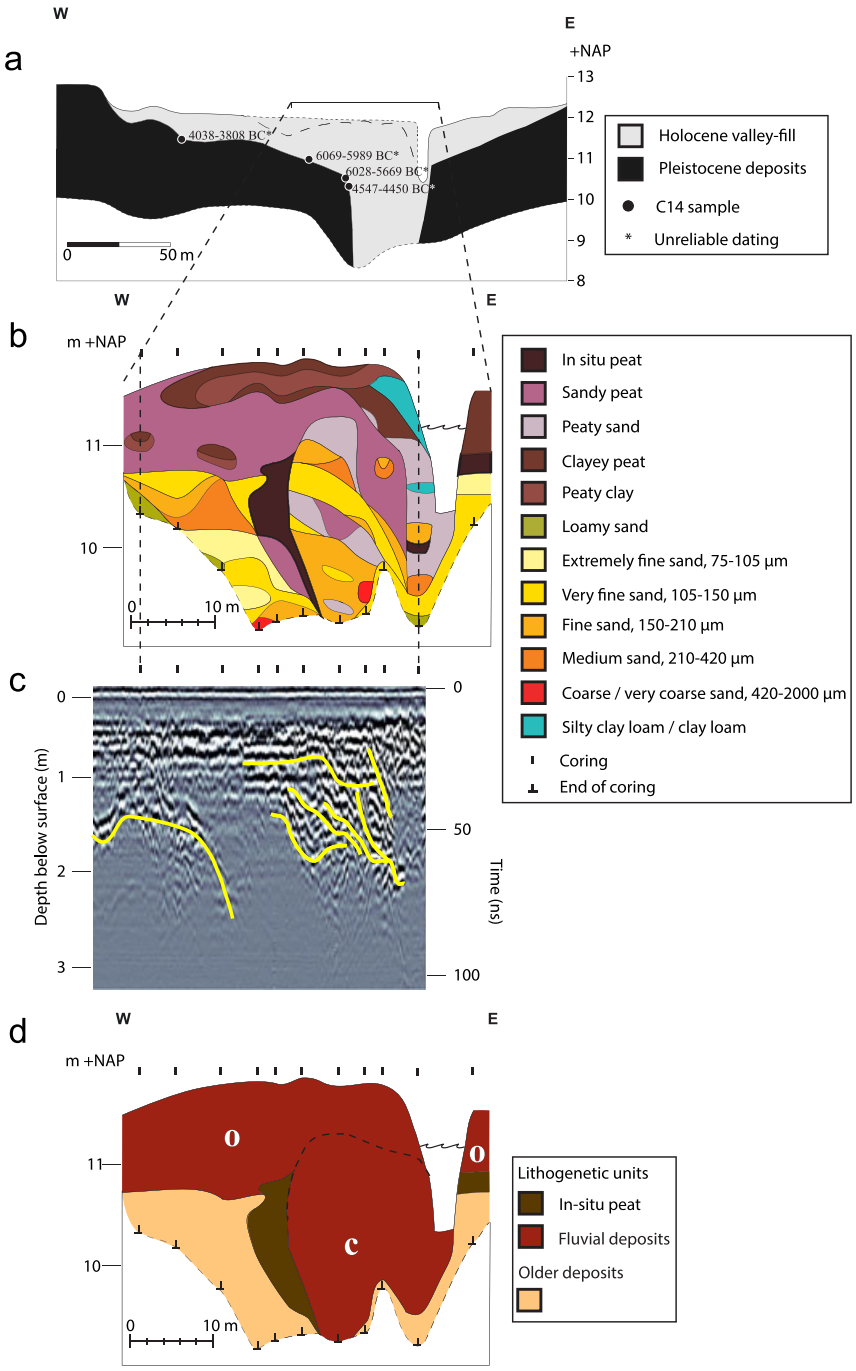

Figure 3. Amen: a) Geological cross-section of the valley (modified after Makaske *et al.*, 2015) b) lithological cross-section of the valley-fill, c) GPR profile of the west side of the stream, d) lithogenetic cross-section of the valley-fill. Letter O indicates overbank deposits. Letter C indicates channel deposits. [Colour figure can be viewed at wileyonlinelibrary.com]

dark grey when sandy, and dark brown to dark grey when clayey. For the peaty facies, clastics are present throughout the entire peat mass. Plant macrofossils are mostly present, but they are relatively small and fragmented compared with the macrofossils in the *in situ* peat unit. Moreover, the macrofossils occur bedded within this unit. The structure is less firm than the *in situ* peat, as the plant macrofossils are not interwoven. The colour of the peat is dark brown.

Channel deposits can sometimes be distinguished within the fluvial deposits unit, when the unit has a low width/thickness ratio, consists of the sandy fraction and contain well developed stratification. Overbank deposits can be distinguished within the fluvial deposits unit, when the fluvial deposits consist of the clayey fraction. In addition, bodies of fluvial deposits with a high width/thickness ratio are interpreted as overbank deposits. These bodies are mostly positioned along the channel deposits, within the matrix of peat. Additional letters 'O' (overbank) and 'C' (channel) are added in the lithogenetic cross-sections when the geometry allows discriminating these lithogenetic sub-units.

The overbank deposits can contain ferruginous concretions, which are irregularly distributed. These concretions were analysed by XRF and consist of 58% iron oxide (Table III); given the clayey and peaty environment, the concretions probably consist of siderite ($FeCO_3$) (Dr Bertil van Os, personal communication, November 2015).

Aeolian deposits consist of clastic sediments varying in texture from medium fine sand to fine sand (150–420 µm). The sand is well sorted, and plant remains are hardly present. The lithogenetic unit is strongly layered. The colour is light to dark

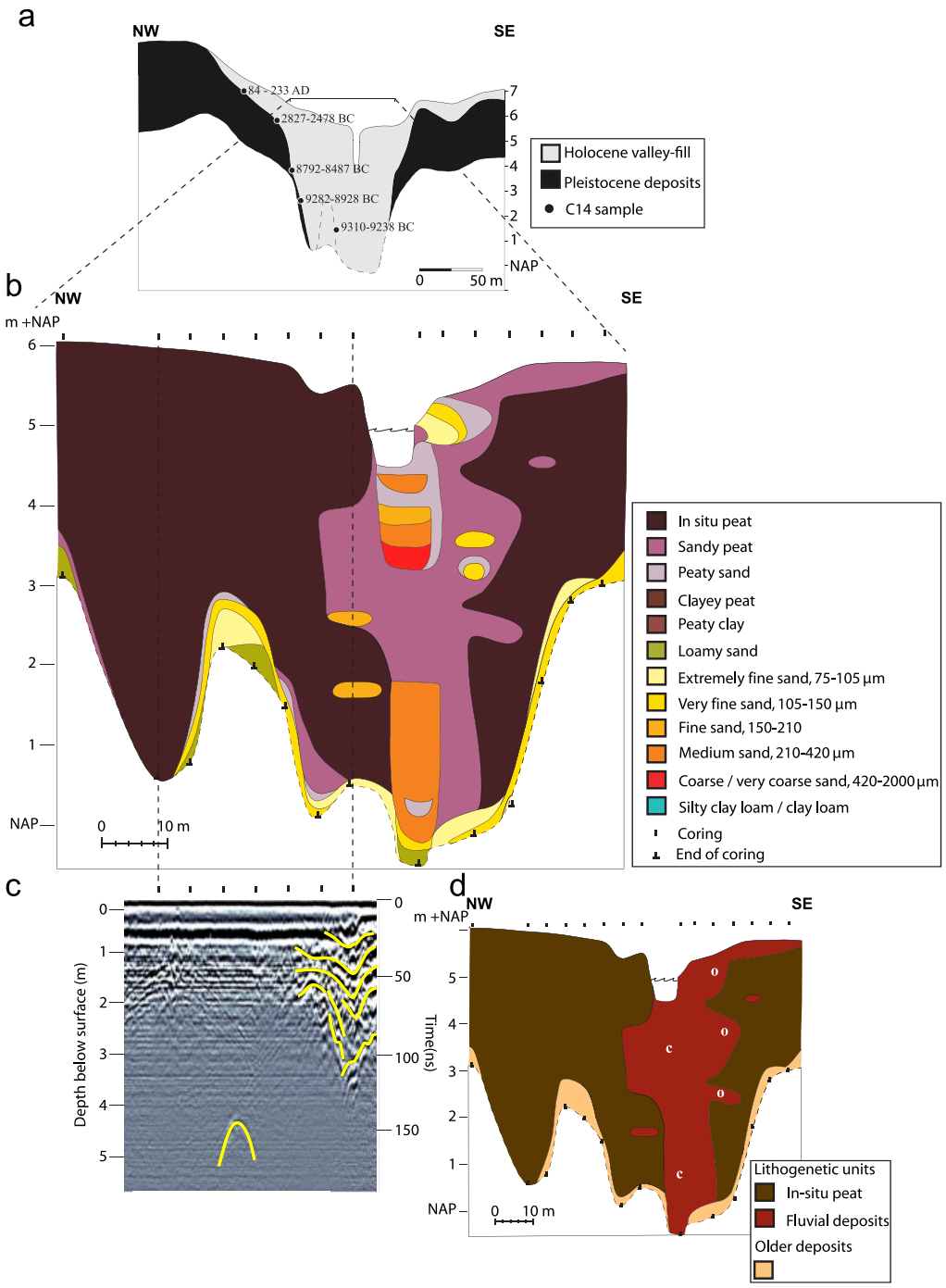

Figure 4. Loon: a) Geological cross-section of the valley (modified after Makaske *et al.*, 2015) b) Lithological cross-section of the valley-fill, c) GPR profile of the west side of the stream, d) lithogenetic cross-section of the valley-fill. Letter O indicates overbank deposits. Letter C indicates channel deposits. [Colour figure can be viewed at wileyonlinelibrary.com]

grey. The unit is only encountered at section Schipborg, where it reaches a thickness up to 4 m, and fills the entire valley on one side of the stream. Beds dip towards the stream with an angle of 15–25°, and strongly compacted *in situ* peat was found below this deposit. The top of the lithogenetic unit consists of topographic highs and lows with 1 to 1.5 m difference in elevation. Elevation differences can be recognized at the surface, and the valley is bordered by dunes. Thick aeolian deposits located at the surface are known in this area as drift-sand deposits (Koster *et al.*, 1993).

Older deposits consist of several lithogenetic units and form the palaeovalley. The unit consists of clastic sediment, varying from fine sand to extremely fine sand (75–210 µm) and are mostly well sorted. The sand may contain low percentages of loam (<10%). At the lowest parts of the palaeovalley the unit can be poorly sorted and contain up to 10% gravel. The unit is easily distinguishable from the other lithogenetic units by its light-grey colour, its strong consolidation, some thin soil formation, and sometimes a sharp transition with the other units. Plant remains are mostly absent. The older deposits largely consist of aeolian sands (coversand) on the valley sides, and fluvial periglacial sands in the valley (De Gans, 1981). No distinction was made, as our interest is in the Holocene deposits of the valley fill.

Cross-sections

At Amen (Figure 3) the palaeovalley is relatively shallow, with a minimum depth of 3 m. The valley-fill mainly consists of fluvial

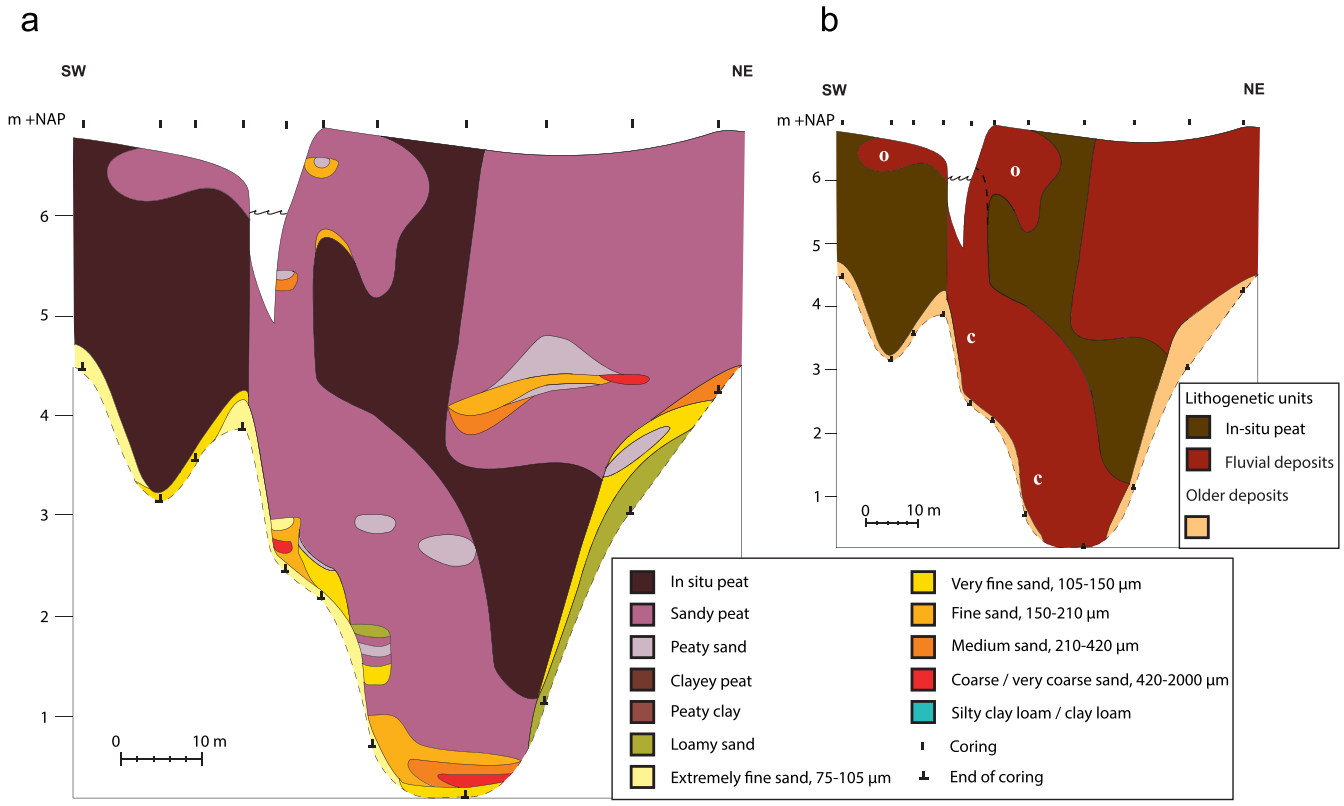

Figure 5. Gasteren1: a) Lithological cross-section of the valley-fill, b) lithogenetic cross-section of the valley-fill. Letter O indicates overbank deposits. Letter C indicates channel deposits. [Colour figure can be viewed at wileyonlinelibrary.com]

deposits, and a small amount of *in situ* peat. The ^{14}C ages of Makaske *et al*. (2015) were in non-stratigraphical order. Our results indicate that this may be due to dating overbank deposits rather than *in situ* peat. At Loon (Figure 4) the channel deposits are located in the middle of the palaeovalley with *in situ* peat on both sides. At Gasteren1 (Figure 5) the channel deposits are located along the southwestern palaeovalley side. Fluvial deposits are also located at the northeastern side of the palaeovalley. From the DEM (Figure 2(c), dashed line) it can be derived that these are remainders of an abandoned stream that is not visible in the field. The palaeovalley in Gasteren2 (Figure 6) is wider than that in Gasteren1. Channel deposits are located in the middle of the palaeovalley below 2.8 m below the surface. Above that level, they are covering the northeastern palaeovalley side. The Schipborg section (Figure 7) differs from the other sections, with the presence of aeolian deposits on top of the peat. Dune deposits (fine sands) are interbedded with fluvial overbank interdune deposits (clay, reworked plant remains) in the lows, similar to that presented in the conceptual model of Langford (1989) and stratigraphy of Langford and Chan (1989). A borehole 100 m farther downstream did not contain this aeolian unit, indicating how local these deposits are (Figure 2(d)). The drift-sand activity seems to have started 2.4 ka ago and was probably strongly related to human activity in the area (Derese *et al*., 2010; Sevink *et al*., 2013; Jager, 2015). Another phase was dated at the start of the Middle Ages, 1.4 ka ago. The age difference to the ^{14}C date below the aeolian deposits is probably the result of wood being taken for the ^{14}C analysis rather than seeds or leaves, resulting in an overestimation of the age (Mook and Streurman, 1983; Törnqvist *et al*., 1992). Other explanations are differential compaction and the slow peat growth rate during this period, which was limited to a few decimetres per thousand years (Makaske *et al*., 2015). At the final section in Kappersbult (Figure 8) the channel deposits are located along the northeastern palaeovalley side. Overbank deposits at this site contain abundant ferruginous concretions (Table III).

Conceptual Model

Stream evolution as a function of valley shape

Until the start of the Bølling-Allerød interstadial (~14.7 ka), peat formation was absent and stream channels were situated on the sandy Pleistocene valley floor. As a result of permafrost conditions in the catchment (De Gans, 1981), streams were probably able to laterally migrate as stream power allowed for lateral erosion of the relatively easily erodible, sandy banks. At a later stage, peat started to form as a result of wetter conditions in the valley (Makaske *et al*., 2015). The oldest ^{14}C date in Kappersbult (KIA_43754, Table II) dates from the Younger Dryas (~12 ka). However, since the ^{14}C date was taken approximately 25 cm above the valley floor, the initial establishment of peat is expected to date from the Bølling-Allerød interstadial (14.7–12.7 ka) when warmer and wetter conditions favoured peat growth (Hoek, 2008).

The peat growth has resulted in changing stream morphodynamics, in a way that depends on the position of the channel in the valley. Here we distinguish between disconnected channels and connected channels. The former are located in the central valley and have peat banks on both sides, while the latter are located at the margin of the floodplain, with a peat bank on the inside and sandy bank on the outside.

Disconnected channel reaches, i.e. those in the centre of the valley, aggrade vertically in response to peat growth. Erosion-resistant peat banks (Micheli and Kirchner, 2002a, b; Gradziński *et al*., 2003; Nanson, 2010; Stenberg *et al*., 2015) are present on both sides of the channel during aggradation, preventing lateral channel migration (Figure 9a-1). This process

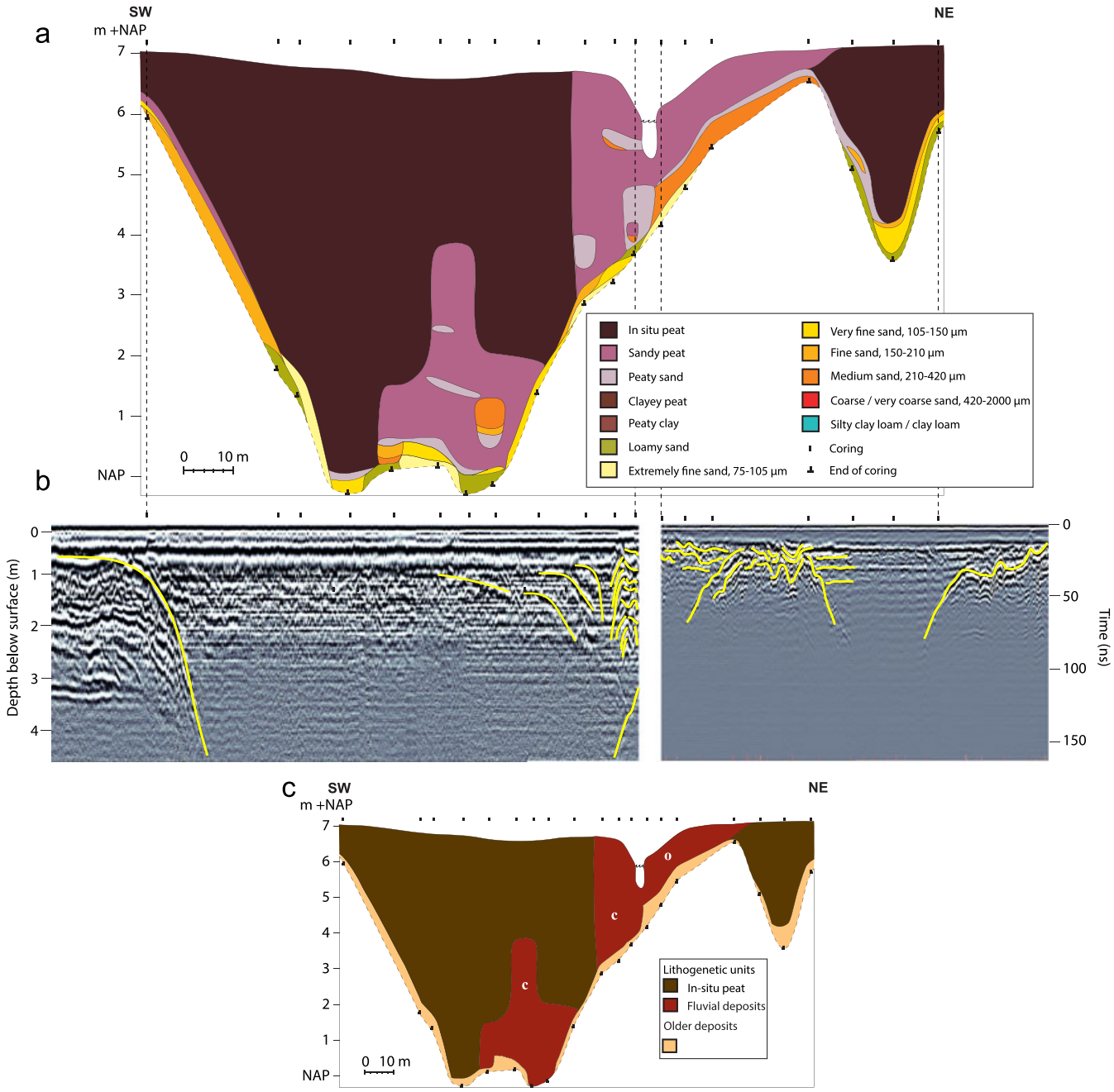

Figure 6. Gasteren2: a) Lithological cross-section of the valley-fill, b) GPR profile of the west and east side of the stream, c) lithogenetic cross-section of the valley-fill. Letter O indicates overbank deposits. Letter C indicates channel deposits. [Colour figure can be viewed at wileyonlinelibrary.com]

can for example be seen in the Loon cross-section (Figure 4). Although the channel bed lithology changed during aggradation, the current stream reach location is vertically in line with the stream reach location at the start of peat growth.

Connected channels, i.e. those touching the valley side, aggrade obliquely along the valley side during the accumulation of peat in the valley (Figure 9a-2). Rajchl and Uličný (2005) used the term oblique aggradation in their work and defined it as 'a combination of lateral migration and aggradation during channel activity, resulting in stacking of channel-fill bodies oblique to general stratification'. Their explanation for oblique aggradation was related to compactional tilting of the underlying peat during the late Oligocene-early Miocene. The underlying cause of oblique aggradation in our study seems related to the differences in resistance to erosion between the peat and the sandy subsurface, with peat having a higher resistance (Micheli and Kirchner, 2002a, b; Stenberg *et al.*, 2015). Because of this difference, channel widening will tend to occur at the sandy valley side. On the other side of the stream, fluvial deposits and vegetation will narrow the channel and deposits will be covered by peat during the aggradation of the valley. The combined effect of these two processes is that the channel is pulled to the valley side. However, the erosion rates seem to be low, resulting in a largely unaffected, relatively symmetrical and uniform shape of the subsurface. Another factor that may affect the adherence of the stream channel to the valley side is groundwater seepage from the higher grounds into the valley (Makaske *et al.*, 2015). The occurrence of seepage and the presence of a sandy substrate are not fully independent. Groundwater seepage can occur in the valley, because the sandy valley side is conductive compared with the underlying tills. Some studies have shown that seepage is an important factor in bank erosion, resulting in unstable banks which can initiate and promote lateral channel migration (Fox *et al.*, 2007, 2010; Van Balen *et al.*, 2008; Eekhout *et al.*, 2013). Seepage does not initiate meandering in the Drentsche Aa, but it may

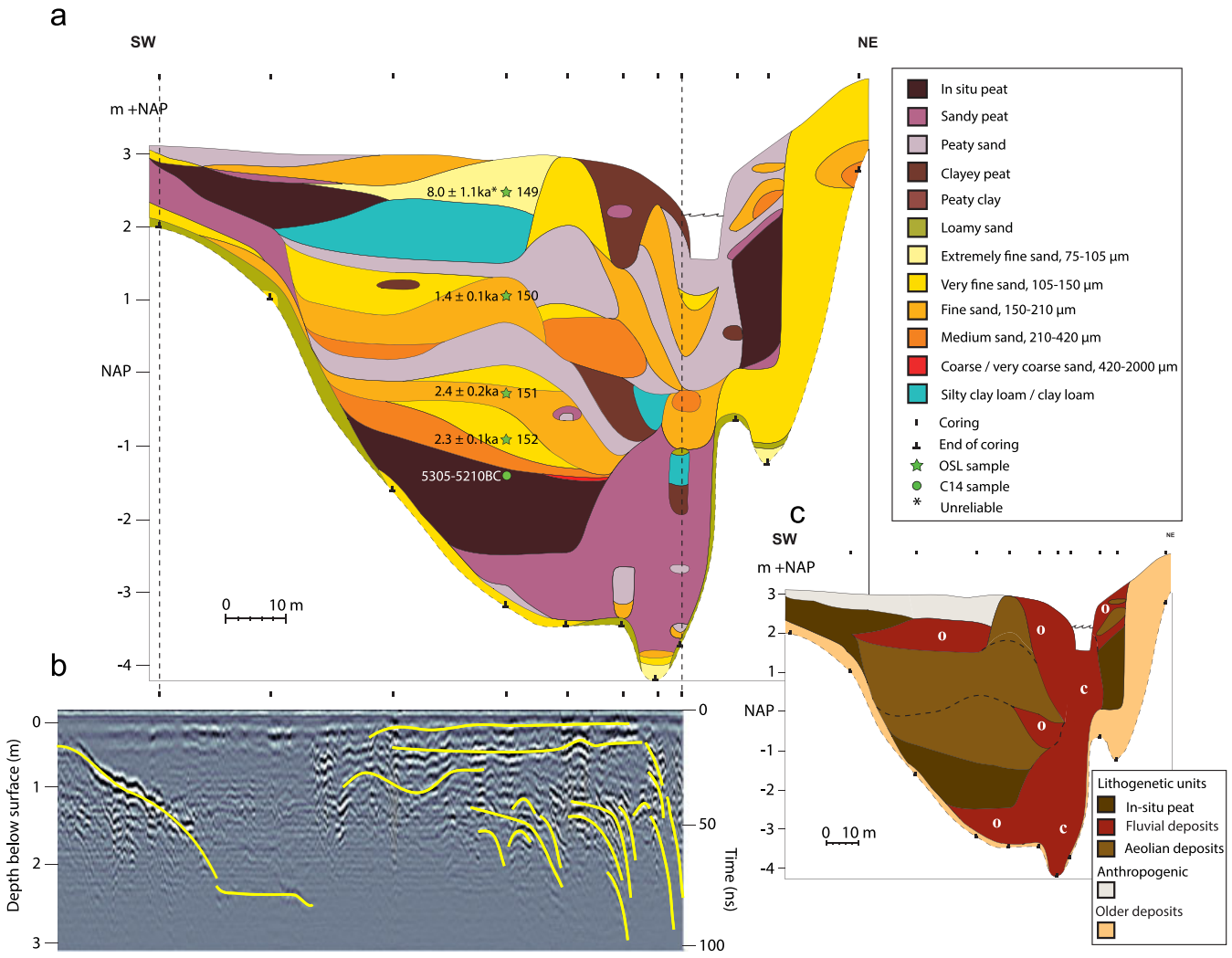

Figure 7. Schipborg: a) Lithological cross-section of the valley-fill, including the OSL and 14C sample locations, b) GPR profile of the west side of the stream, c) lithogenetic cross-section of the valley-fill. Letter O indicates overbank deposits. Letter C indicates channel deposits. [Colour figure can be viewed at wileyonlinelibrary.com]

enhance the process of oblique aggradation by lowering the resistance to erosion of the valley side. In settings with raised peat bogs the relief may be a third factor. Here, discharge will be concentrated at topographic lows at the margins of the convex bogs, and streams will aggrade obliquely when the bog expands (Ingram and Gore, 1983, p.132). However, this setting differs from the Drentsche Aa where peat growth is groundwater-controlled (Makaske *et al.*, 2015), also shown by the presence of siderite and iron oxides at the section Kappersbult (Curtis and Coleman, 1986). Therefore, our setting lacks the convex shape typical for raised bogs, and surface relief is expected to play a minor role in the oblique aggradation process that we document.

The process of oblique aggradation can be seen in the Gasteren1, Gasteren2, Schipborg and Kappersbult cross-sections (Figures 5–7 and 8, respectively). Although Schipborg differs from these other sections, because sand banks seem to have been present on both sides of the stream (Figure 7(a)), oblique aggradation also occurred here. Before drift-sand was deposited (2.4 ka) peat had a thickness of 6 to 7 m, reaching the current surface level, comparable to the cross-sections at Kappersbult and Loon where ^{14}C datings are present (Table II). Channel deposits were located along the northeastern palaeovalley side. When the drift-sand was deposited, the peat was compacted 3 to 4 m by the weight of the deposits, but this occurred after the oblique aggradation had taken place.

The development of peat is closely associated with the groundwater level (Clymo, 1991). As aggradation continues during the Holocene, the groundwater level can rise above the valley sides. As a result, the peat can overtop the subsurface topography and lie on top of the valley sides. If peat overtops the valley, this may cause streams to disconnect from the valley side and continue to aggrade vertically rather than obliquely. This situation is shown in Figure 9a-3, and may explain the transition from oblique to vertical aggradation shown for Gasteren1 and Schipborg (Figures 5 and 7). The contrary transition does also occur. A disconnected aggrading channel can become connected to the valley side due to an avulsion, and aggrade obliquely from then on. This is shown in Figure 9a-4, and may explain the transition from vertical to oblique aggradation for Gasteren2 (Figure 6(c)).

There are several conditions facilitating oblique aggradation. We expect the process of oblique aggradation to be a function of the valley side slope and rate of peat development. Oblique aggradation is possible if the valley side is not sufficiently stabilized by peat prior to exposure to flowing water of the stream. For example, if the valley side slope is very gentle, the stream can become disconnected from the valley side, since peat can grow on both sides of the stream. A high peat growth rate might enhance the stream becoming disconnected. However, from our data it is impossible to define thresholds for the valley side slope and peat growth rate for oblique aggradation to

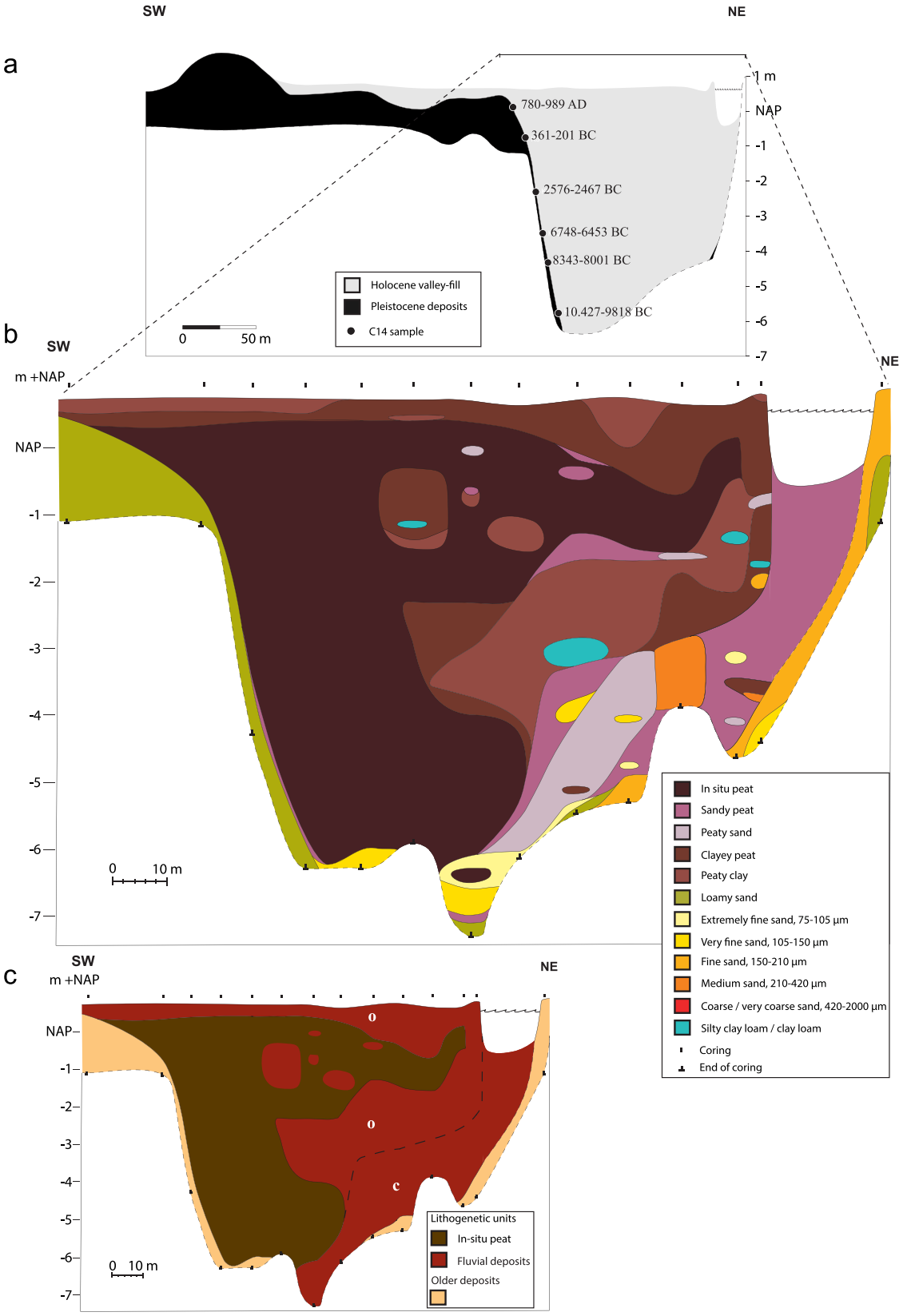

Figure 8. Kappersbult: a) Geological cross-section of the valley (modified after Makaske *et al.*, 2015), b) lithological cross-section of the valley-fill, c) lithogenetic cross-section of the valley-fill. Letter O indicates overbank deposits. Letter C indicates channel deposits. Actual channel depth is an estimation of the average channel depth. [Colour figure can be viewed at wileyonlinelibrary.com]

occur. Oblique aggradation occurred over a wide range of valley side slopes of 3 to 28°. Moreover, the peat growth rates and therefore the aggradation rates changed over time in the Drentsche Aa valley (Makaske *et al.*, 2015), but did not seem to affect the oblique aggradation.

Effects on stream planform

Applying the previously described mechanisms to the channel planform shows that the sinuous planform is partly inherited from the period before peat started to grow and fixed the

Table I. OSL results from a coring 30 m west of the stream in Schipborg (Figure 7). Lat,Lon (RD): 240983,565193

Sample code	Material	Depth **(m + NAP)**	Palaeodose **(Gy)**	Dose rate **(Gy/ka)**	Age **(ka)**
NCL2315**149***	Anthropogenic	2.50	9.8 ± 1.2	1.22 ± 0.07	8.0 ± 1.07
NCL2315**150**	Aeolian	1.10	1.4 ± 0.1	1.01 ± 0.06	1.4* ± 0.06
NCL2315**151**	Aeolian	–0.25	1.8 ± 0.1	0.79 ± 0.03	2.3* ± 0.08
NCL2315**152**	Aeolian	–0.85	1.9 ± 0.1	0.78 ± 0.03	2.4 ± 0.14

*Unreliable dating, this sample has been anthropogenically influenced.

Table II. ^{14}C dating results

Sample code	Material	Depth **(m + NAP)**	^{14}C age **(a BP)**	Age **(a)**	Age **BC/AD**	Lat/Lon (RD)
KIA-43998*	Wood and bark	11.45	5149 ± 34	4038–3808	BC	238.099 / 551.890
KIA-43999*	Wood and bark	11.13	7166 ± 35	6069–5989	BC	238.157 / 551.908
KIA-44000*	Wood and bark	10.61	6979 ± 104	6028–5669	BC	238.173 / 551.914
KIA-44001*	Wood and bark	10.44	5668 ± 30	4547–4450	BC	238.176 / 551.915
KIA-43745	Plant remains	11.45	1854 ± 32	84–233	AD	237.992 / 559.305
KIA-43746	Plant remains	5.85	4042 ± 27	2827–2478	BC	238.011 / 559.239
KIA-43747	Seeds	3.82	9384 ± 57	8792–8487	BC	238.018 / 559.275
KIA-43748	Bark	2.63	9717 ± 46	9282–8928	BC	238.023 / 559.270
KIA-43749	Bark	1.46	9811 ± 39	9310–9238	BC	238.041 / 559.248
KIA_43750	Seeds	0.10	1135 ± 42	780–989	AD	237.669 / 571.553
KIA_43751	Wood	–0.77	2206 ± 25	361–201	BC	237.675 / 571.557
KIA_43752	Buds	–2.32	3999 ± 33	2576–2467	BC	237.680 / 571.559
KIA_43753	Reed	–4.32	9043 ± 39	8343–8001	BC	237.687 / 571.562
KIA_43754	Seeds	–5.76	10266 ± 58	10.178–9881	BC	237.692 / 571.565
KIA_43755	Reed	–3.48	7757 ± 69	6748–6504	BC	237.684 / 571.561
GrA64718	Wood	–1.25	6250 ± 40	7.3–7.2	BC	240.983 / 565.193

*Unreliable dating, since this sample turned out to be fluvial reworked peat.

Table III. XRF analysis results of concretion sample

Type	Amount (%)
SiO_2	25
CaO	1.60
P_2O_5	0.35
K_2O	0.345
Al_2O_3	2.57
TiO_2	0.069
Fe_2O_3	58
MnO	2.39
Bal	8.78

channel reaches. In addition, the sinuous stream planform is partly the result of the combined processes of vertical and oblique aggradation, alternately pulling the stream reaches to the one or the other, opposed valley side (Figure 9(b)). Moreover, the floodplain of the stream widens as a result of peat growth in a V-shaped valley. Adherence of stream reaches to the valley sides, in combination with floodplain widening, results in a stream that is stretched out resulting in increased sinuosity. Our conceptual model shows that the palaeovalley shape is essential for the formation of the current stream planform and floodplain. The palaeovalley shape controls how much the stream planform is stretched out in the case of a connected stream, controls whether a stream can become disconnected as a result of peat growth on top of the valley side, and controls the width of the floodplain. The stretching occurred mainly in the first period of the aggradation, when the stream was still connected to the valley side. The process will stop if the peat overtops the valley sides, because the stream cannot be connected anymore from that point onwards. The stretching of the stream results in a very distinctive and unique planform, with rectangular bends and relatively straight reaches that either follow the palaeovalley sides, or cross the palaeovalley. Such planforms are present along the entire length of the Drentsche Aa (Figure 1 and 2). This planform is characteristic for the oblique aggradation process, and different from more circular bends in sinuous planforms that are the result of the process of lateral migration of meandering rivers (Lobeck, 1939; Leopold and Wolman, 1960). Figure 9(c) schematically illustrates both planforms.

In Gasteren1 (Figure 5) an abandoned channel is located parallel to the current channel. The abandoned channel can also be seen on the DEM showing a channel-shaped low at this location (Figure 2(c)). The abandoned channel can be interpreted as an old tributary, by tracing back the upstream channel reaches on the DEM. The DEM reveals several other inactive channels located parallel to the current active channel within the Drentsche Aa valley. However, these are not defined as elements of an anastomosing stream system (Makaske, 2001), as for instance in the Narew River in Poland where channels are interconnected (Gradziński *et al.*, 2003). From the DEM it can be derived that these parallel channels are former tributaries that run parallel to the main channel for some distance, separated by erosion-resistant peat in between the channels. Nonetheless, some tributary channels enabled avulsions affecting the connectivity of the stream to the valley side, as well as the stream planform (Figure 9a-4). The occurrence of avulsions can be derived

from the cross-sections at Gasteren (Figures 5 and 6). An avulsion between Gasteren1 and Gasteren2 led to a shift of the main channel in the centre of the valley to the northeastern valley side by annexation of the lower reach of the tributary. However, the avulsion frequency is probably low, because of the low amount of tributary channels present in the Drentsche Aa valley. Our findings are in line with Gradziński *et al*. (2003), who also found that avulsions are infrequent processes in peatlands.

Discussion

Landscape evolution in low-energy streams

Although the conceptual model of oblique aggradation presented here is based on data from the Drentsche Aa, we expect it to be applicable to the morphological development of other streams in similar settings. For example, the distinctive planform with rectangular bends and straight stretches

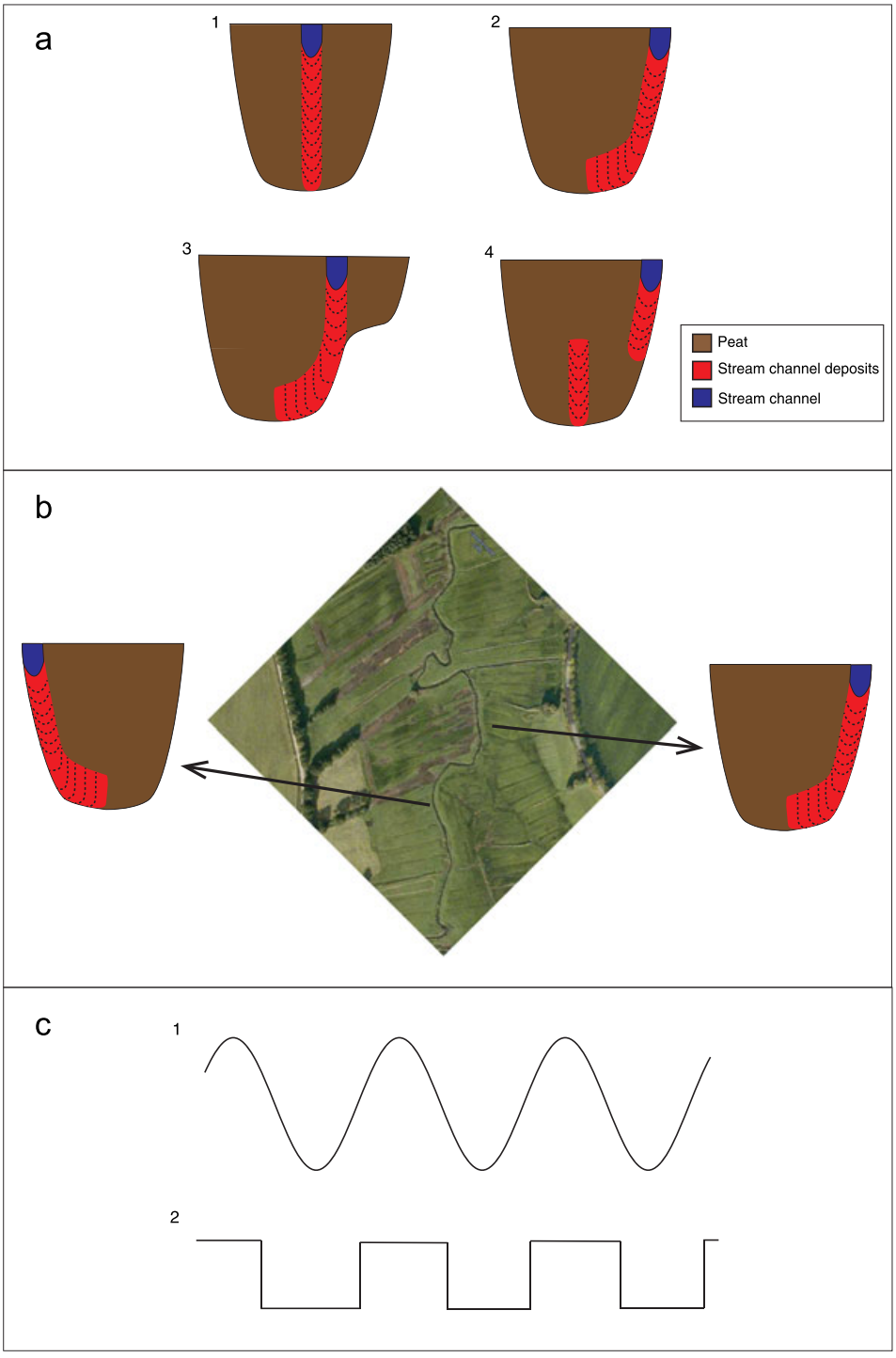

Figure 9. Conceptual model of oblique aggradation in a peat-filled valley, resulting in the rectangular, sinuous planform. a) Simplified, schematic cross-sections illustrating different processes that affect the channel planform and morphology in a Holocene valley filled up with peat. 1) An aggrading disconnected channel, 2) a connected channel obliquely aggrading along the valley side, 3) a connected channel changing to a disconnected channel because it overtops the valley, 4) a disconnected channel changing to a connected channel as the result of an avulsion. b) A sketch of the sinuous planform formation by oblique aggradation. c) A sketch of 1) a sinuous planform as a result of lateral migration, 2) a rectangular sinuous planform as a result of oblique aggradation.

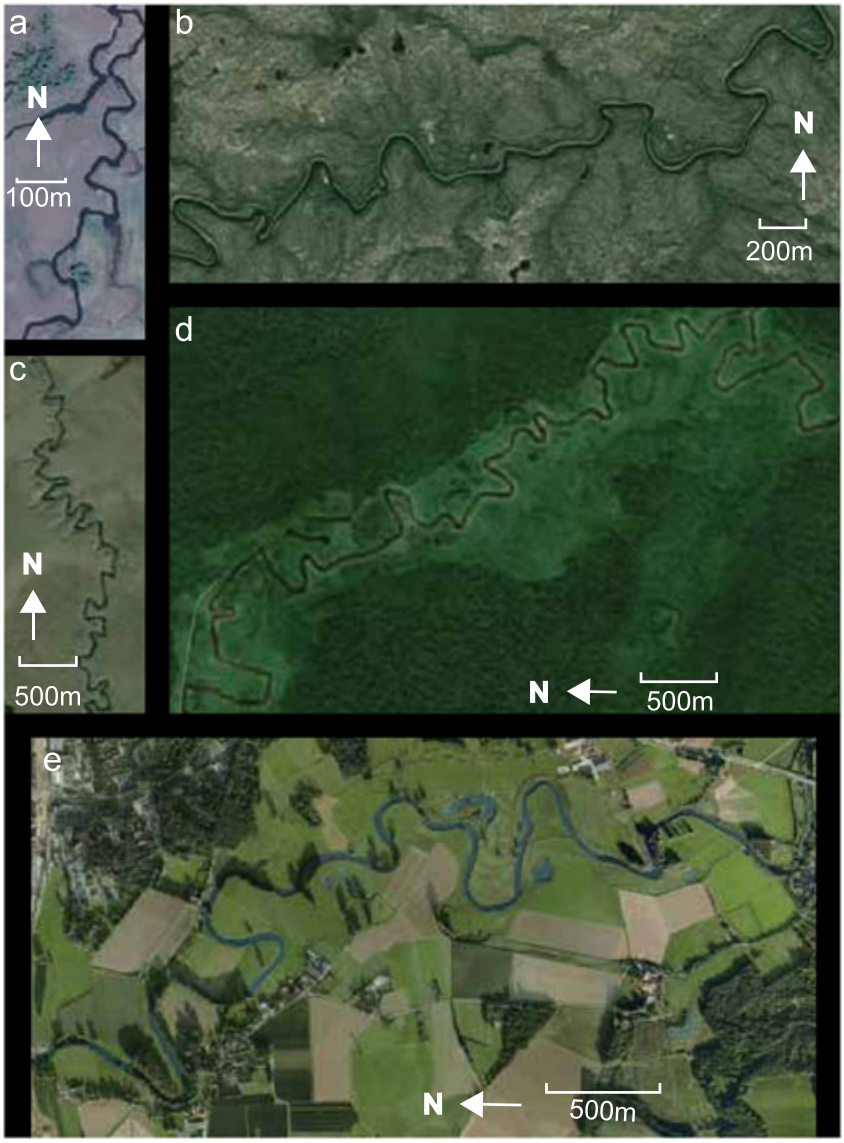

Figure 10. Stream planforms throughout the world. a) The Narew River in Poland (53°06′17.9″N 22°48′33.7″E); b) a stream draining in the Hudson Bay near Churchill (58°16′09.8″N 95°43′18.4″W); c) a stream near Taman National Park in Indonesia (1°03′05.7″N 112°21′44.5″E); d) a tributary of Uele in Siberia (72°32′24.3″N 118°04′23.0″E); e) the Roer in The Netherlands 51° 9′42.80″N 6° 0′1.43″E). Source: Google Earth, 2016. [Colour figure can be viewed at wileyonlinelibrary.com]

(Figure 9(c)) can be used to identify streams where oblique aggradation may be a dominant mechanism in stream valley reaches with a dominantly organic subsoil. Similar planform characteristics were found for some channel reaches of the anastomosing Narew River in Poland (Figure 10(a)). Gradziński *et al*. (2003) found that peat growth started here at some locations in the Middle Holocene, reaching thicknesses up to 4 m on top of a glacio-fluvial sandy subsurface. They also found that most channel reaches have a low sinuosity, typical for anastomosing rivers (Makaske, 2001). However, Gradziński *et al*. (2003) were not able to explain the presence of channel reaches with a high sinuosity. They also found that these channel reaches are lacking point bars and have not changed planform or position for over 100 years, as appears from comparison with historical maps of 1886. Our conceptual model may explain the typical planform of the Narew River. Because peat aggraded above the palaeovalley margins, the underlying palaeovalley structures guiding the oblique aggradation mechanism cannot be recognized nowadays and the surface topography is flat.

An exploratory inventory based on satellite imagery (Google Earth) of remote peatland areas with minimal human disturbance provided several other examples of streams with the distinctive rectangular planform, similar to that found in the Drentsche Aa. Examples include streams in vast peatland areas in Siberia, Canada, and Indonesia where peat has grown for the past millennia (Botch *et al*., 1995; Page *et al*., 1999; Bridgham *et al*., 2006; Dyke and Sladen, 2010; Vermeulen *et al*., 2014) (Figure 10(b)–(d)). The planforms of these streams differ from more rounded planforms of alluvial meandering streams, e.g. de Roer in The Netherlands (Figure 10(e)) (Wilde and Tanzer, 1965). Although palaeohydrological information on the identified streams in peatlands is lacking, we suggest that it is highly likely that oblique aggradation caused the planform formation, similar to the Narew River.

We propose that our conceptual model of oblique aggradation is applicable when certain preconditions are present. First, an aggrading setting is needed, which is often associated with peat growth. Peat forms as a result of permanently high groundwater levels. Controlling factors of peat growth are climate change and base level rise. Both may result in rising regional groundwater levels. A second precondition is relief. Without relief, streams will be disconnected and oblique aggradation cannot occur. Thirdly, the valley side should have a lower

erodibility than the valley fill. If both banks are equally erodible, connected streams will not adhere to the valley side and oblique aggradation will not occur. Taking these preconditions into account, oblique aggradation can also occur in different stream settings from those presented in this study, explaining the sinuous planform. For instance, a detailed sedimentological study by Makaske *et al*. (2002, p. 1054) revealed oblique aggradation in the upper Columbia River. In this case, the oblique aggradation was not related to peat growth, but rather the result of one bank being more erodible than the opposed bank during aggradation of the system. This example corroborates that oblique aggradation is a consequence of differences in erosion-resistance of opposing banks. Therefore, oblique aggradation can also occur in aggrading stream valleys with a clayey valley-fill that also has a relatively high resistance to erosion (Grissinger, 1982; Thorne, 1982). Obliquely aggrading rivers with a clayey bank were also observed by Berendsen and Stouthamer (2000). They found that the meandering rivers Rhine and Meuse between approximately 6000–2500 BP tended to adhere to the sandy edges of the Late Weichselian palaeovalley rather than the central valley, which contains many clay and peat layers. However, the sinuous planform of these rivers is formed by meandering, since a higher stream power results in the ability of a river to meander in spite of erosion-resistant banks (Kleinhans and Van den Berg, 2011). Therefore, oblique aggradation is expected to have a larger impact on the planform of low-energy rivers than on the planform of high-energy rivers.

In different stream settings, the Stable-Bed-Aggrading-Banks model by Brown and Keough (1992) and Brown *et al*. (1994) might explain the presence of a sinuous planform in laterally stable streams. This model shows that sinuous stream planforms can be inherited from past fluvial regimes when the stream had enough stream power to form a sinuous planform. However, where oblique aggradation results in an increase of sinuosity over time, the stable-bed-aggrading-bank model results in preservation of sinuosity.

Lessons for stream restoration

The palaeohydrological context of streams provides valuable information for water managers to identify realistic stream restoration goals. Currently, stream restoration often fails, due to the lack of a scientific context (Wohl *et al*., 2005) and stream restoration practices (e.g. stream re-meandering) are often implemented without having set clear goals or states of success (McMillan and Vidon, 2014). It has been argued that reference states should not be used as a goal in stream restoration projects, since streams are dynamic and change over time so previous states may be impossible to return to (Dufour and Piégay, 2009). Instead, it has been argued that we should learn from the processes that result in stream dynamics and account for these processes in the restored stream (Kondolf, 2006; Brierley and Fryirs, 2009, 2015). Makaske and Maas (2015) suggested designing new stream channels based on calculations of the hydraulic and planform geometry that fit the current stream power rather than copying these aspects from historic maps. However, the planform of a peatland stream such as the Drentsche Aa has changed little over the last thousands of years and bears little relation to the hydrology of the system and limited changes thereof. Therefore historical maps provide excellent input to design the stream planform in peatland streams.

Some stream restoration projects in peatlands involve restoring dispersed wetland systems rather than re-designing the stream channel. An example of a historic dispersed wetland system, or 'swampy meadow' (Mactaggart *et al*., 2008), was found in south-eastern Australia. Here the dispersed wetland system was incised by a stream following human colonization and land use changes (Prosser *et al*., 1994; Nanson, 2009). For the Drentsche Aa system, we found no evidence of a wetland without a channel. In contrast, all stratigraphic cross-sections show evidence of channel deposits at all stratigraphic levels, although we are aware that stratigraphic layers without a channel might have existed and been incised by a channel at a later stage. From our data and a previous study (Makaske *et al*., 2015) there are no indications of specific incisional phases, although again minor phases of incision or denudation cannot be excluded. This finding contrasts with previous ideas of natural streams in similar lowland settings. Broothaerts *et al*. (2013) and Lespez *et al*. (2015) related the presence of peat in valley systems to dispersed wetland systems. Our study shows that stream channels can be identified within peat, but that such differentiation requires a very dense core spacing combined with detailed lithogenetic identification. We propose that dispersed wetland systems are not the natural state of low-energy stream valleys such as the Drentsche Aa, although we cannot rule out that dispersed wetland systems existed in the upper branches of the stream system, where the stream power is too low to actually form a channel.

Conclusions

We identify oblique aggradation as a key process leading to highly sinuous planforms in peat-filled valley systems. Oblique aggradation may occur in aggradational settings where the valley side consists of material that is more easily erodible than the (organic) valley fill. The stream becomes literally stretched out over time owing to a combination of floodplain widening and stream reaches aggrading obliquely along opposed valley sides. This novel conceptual model for stream evolution may explain rectangular, sinuous planforms observed for other peatland systems from satellite imagery, and may also be applicable to other settings where opposed banks have differences in erosion resistance. Our explanation of the sinuosity of low-energy streams in the absence of lateral migration supports water managers in stream channel design in the context of stream restoration projects.

Acknowledgement—This research is part of the research program RiverCare, supported by the Dutch Technology Foundation STW, which is part of the Netherlands Organization for Scientific Research (NWO), and which is partly funded by the Ministry of Economic Affairs under grant number P12–14 (Perspective Programme). The authors would like to thank the following fellow fieldworkers for their help: Jos Candel, Bas Nabers, and Foeke Menting. The manuscript has benefited greatly from reviews by Kim Cohen and one anonymous reviewer. Dr Bertil van Os is thanked for his help with the XRF-analysis. Erna Voskuilen, Dr Benny Guralnik, Alice Versendaal and Maud van Soest are thanked for their help with the OSL analysis. Peter Paul Schollema is thanked for introducing the study area, Philip Wenting for his help with the GNSS and GPR, and Harry Offringa for the permission of Staatsbosbeheer to do fieldwork in the nature area. Gilbert Maas, Dr Ype van der Velde and Dr Jelmer Nijp are thanked for the open discussions on the concepts.

References

Aitken MJ. 1985. *Thermoluminescence Dating*. Academic Press: London.

Berendsen HJ, Stouthamer E. 2000. Late Weichselian and Holocene palaeogeography of the Rhine–Meuse delta, The Netherlands. *Palaeogeography Palaeoclimatology Palaeoecology* **161**: 311–335.

Berendsen HJ, Stouthamer E. 2001. Palaeogeographic development of the Rhine-Meuse delta, the Netherlands, Koninklijke van Gorcum.

Bos IJ, Busschers FS, Hoek WZ. 2012. Organic-facies determination: a key for understanding facies distribution in the basal peat layer of the Holocene Rhine-Meuse delta, The Netherlands. *Sedimentology* **59**: 676–703.

Botch MS, Kobak KI, Vinson TS, Kolchugina TP. 1995. Kolchugina, Carbon pools and accumulationin peatlands of the former Soviet Union. *Global Biogeochem. Cycles* **9**: 37–46.

Bøtter-Jensen L, Andersen C, Duller G, Murray A. 2003. Developments in radiation, stimulation and observation facilities in luminescence measurements. *Radiation Measurements* **37**: 535–541.

Bridgham SD, Megonigal JP, Keller JK, Bliss NB, Trettin C. 2006. The carbon balance of North American wetlands. *Wetlands* **26**: 889–916. DOI:10.1672/0277-5212(2006)26[889:tcbona]2.0.co;2.

Brierley G, Fryirs K. 2009. Don't fight the site: three geomorphic considerations in catchment-scale river rehabilitation planning. *Environmental Management* **43**: 1201–1218.

Brierley GJ, Fryirs K. 2000. River styles, a geomorphic approach to catchment characterization: implications for river rehabilitation in Bega catchment, New South Wales, Australia. *Environmental Management* **25**: 661–679.

Brierley GJ, Fryirs KA. 2015. The use of evolutionary trajectories to guide 'moving targets' in the management of river futures. *River Research and Applications*. DOI:10.1002/rra.2930.

Bronk Ramsey C. 2009. OxCal Program v4.2. Online: http://www.rlaha.ox.ac.uk/orau/oxcal.html.

Broothaerts N, Verstraeten G, Kasse C, Bohncke S, Notebaert B, Vandenberghe J. 2014. From natural to human-dominated floodplain geoecology – a Holocene perspective for the Dijle catchment, Belgium. *Anthropocene* **8**: 46–58. DOI:10.1016/j.ancene.2014.12.001.

Broothaerts N, Verstraeten G, Notebaert B, Assendelft R, Kasse C, Bohncke S, Vandenberghe J. 2013. Sensitivity of floodplain geoecology to human impact: a Holocene perspective for the headwaters of the Dijle catchment, central Belgium. *The Holocene* **23**: 1403–1414. DOI:10.1177/0959683613489583.

Brown A, Keough M. 1992. Holocene floodplain metamorphosis in the Midlands, United Kingdom. *Geomorphology* **4**: 433–445.

Brown A, Keough M, Rice R. 1994. Floodplain evolution in the East Midlands, United Kingdom: the Lateglacial and Flandrian alluvial record from the Soar and Nene valleys. *Philosophical Transactions of the Royal Society of London A: Mathematical, Physical and Engineering Sciences* **348**: 261–293.

Busschers FS, Van Balen RT, Cohen KM, Kasse C, Weerts HJT, Wallinga J, Bunnik FPM. 2008. Response of the Rhine–Meuse fluvial system to Saalian ice-sheet dynamics. *Boreas* **37**: 377–398. DOI:10.1111/j.1502-3885.2008.00025.x.

Clymo RS. 1991. Peat growth. *Quaternary Landscapes*: 76–112.

Cunningham A, Wallinga J, Minderhoud P. 2011. Expectations of scatter in equivalent-dose distributions when using multi-grain aliquots for OSL dating. *Geochronometria* **38**: 424–431.

Cunningham AC, Wallinga J. 2010. Selection of integration time intervals for quartz OSL decay curves. *Quaternary Geochronology* **5**: 657–666.

Cunningham AC, Wallinga J. 2012. Realizing the potential of fluvial archives using robust OSL chronologies. *Quaternary Geochronology* **12**: 98–106.

Curtis CD, Coleman ML. 1986. Controls on the precipitation of early diagenetic calcite, dolomite and siderite concretions in complex depositional sequences. In *Roles of Organic Matter in Sediment Diagenesis*, Gautier DL (ed). SEPM Spec. Publ., **38**: 23–33.

De Gans W. 1981. The Drentsche Aa Valley System: A Study in Quaternary Geology. Dissertation, Vrije Universiteit van Amsterdam.

Derese C, Vandenberghe D, Eggermont N, Bastiaens J, Annaert R, Van den haute P. 2010. A medieval settlement caught in the sand: optical dating of sand-drifting at Pulle (N Belgium). *Quaternary Geochronology* **5**: 336–341. DOI:10.1016/j.quageo.2009.01.003.

Dufour S, Piégay H. 2009. From the myth of a lost paradise to targeted river restoration: forget natural references and focus on human benefits. *River Research and Applications* **25**: 568–581.

Dyke LD, Sladen WE. 2010. Permafrost and peatland evolution in the northern Hudson Bay Lowland. *Manitoba. Arctic*: 429–441.

Eekhout J, Fraaije R, Hoitink A. 2014. Morphodynamic regime change in a reconstructed lowland stream. *Earth Surface Dynamics* **2**: 279.

Eekhout J, Hoitink A, Makaske B. 2013. Historical analysis indicates seepage control on initiation of meandering. *Earth Surface Processes and Landforms* **38**: 888–897.

Eekhout JP, Hoitink AJ, de Brouwer JH, Verdonschot PF. 2015. Morphological assessment of reconstructed lowland streams in the Netherlands. *Advances in Water Resources* **81**: 161–171.

Fox GA, Heeren DM, Wilson GV, Langendoen EJ, Fox AK, Chu-Agor ML. 2010. Numerically predicting seepage gradient forces and erosion: Sensitivity to soil hydraulic properties. *Journal of hydrology* **389**: 354–362.

Fox GA, Wilson GV, Simon A, Langendoen EJ, Akay O, Fuchs JW. 2007. Measuring streambank erosion due to groundwater seepage: correlation to bank pore water pressure, precipitation and stream stage. *Earth Surface Processes and Landforms* **32**: 1558–1573.

Galbraith RF, Roberts RG, Laslett G, Yoshida H, Olley JM. 1999. Optical dating of single and multiple grains of quartz from Jinmium rock shelter, northern Australia: Part I, experimental design and statistical models. *Archaeometry* **41**: 339–364.

Grabowski RC, Surian N, Gurnell AM. 2014. Characterizing geomorphological change to support sustainable river restoration and management. *Wiley Interdisciplinary Reviews: Water* **1**: 483–512. DOI:10.1002/wat2.1037.

Gradziński R, Baryła J, Doktor M, Gmur D, Gradziński M, Kędzior A, Paszkowski M, Soja R, Zieliński T, Żurek S. 2003. Vegetation-controlled modern anastomosing system of the upper Narew River (NE Poland) and its sediments. *Sedimentary Geology* **157**: 253–276. DOI:10.1016/S0037-0738(02)00236-1.

Grissinger E. 1982. Bank erosion of cohesive materials. *Gravel-Bed Rivers* 273–287.

Guérin G, Mercier N, Adamiec G. 2011. Dose-rate conversion factors: update. *Ancient TL* **29**: 5–8.

Gurnell A. 2014. Plants as river system engineers. *Earth Surface Processes and Landforms* **39**: 4–25. DOI:10.1002/esp.3397.

Gurnell A, Bussettini M, Camenen B, González del Tánago M, Grabowski R, Hendriks D, Henshaw A, Latapie A, Rinaldi M, Surian N. 2014. A hierarchical multi-scale framework and indicators of hydromorphological processes and forms. Deliverable 2.1, Part 1, of REFORM (REstoring rivers FOR effective catchment Management), a collaborative project (large-scale integrating project) funded by the European Commission within the 7th Framework Programme under Grant Agreement 282656.

Hoek WZ. 2008. The last glacial–interglacial transition. *Episodes* **31**: 226–229.

Ingram H, Gore A. 1983. *Mires: Swamp, Bog, Fen, and Moor.* Elsevier Science, Amsterdam, The Netherlands, 67–150.

Jager S. 2015. Van hunebedbouwer tot Drent - Bewaoning en landgebruik tot de Vroege Middeleeuwen, Landschapsbiografie van de Drentsche Aa: Assen, Koninklijke Van Gorcum,54–81.

Jurmu MC. 2002. A morphological comparison of narrow, low-gradient streams traversing wetland environments to alluvial streams. *Environmental Management* **30**: 0831–0856.

Jurmu MC, Andrle R. 1997. Morphology of a wetland stream. *Environmental Management* **21**: 921–941.

Kleinhans MG, Schuurman F, Bakx W, Markies H. 2009. Meandering channel dynamics in highly cohesive sediment on an intertidal mud flat in the Westerschelde estuary, the Netherlands. *Geomorphology* **105**: 261–276.

Kleinhans MG, Van den Berg JH. 2011. River channel and bar patterns explained and predicted by an empirical and a physics-based method. *Earth Surface Processes and Landforms* **36**: 721–738.

Kondolf GM. 2006. River restoration and meanders. *Ecology and Society* **11**: 42.

Kondolf GM, Piégay H, Landon N. 2002. Channel response to increased and decreased bedload supply from land use change: contrasts between two catchments. *Geomorphology* **45**: 35–51. DOI:10.1016/S0169-555X(01)00188-X.

Kondolf GM, Piégay H, Schmitt L, Montgomery DR. 2003a. Geomorphic classification of rivers and streams. *Tools in Fluvial Geomorphology*: 133–158.

Kondolf GM, Piégay H, Sear D. 2003b. Integrating geomorphological tools in ecological and management studies. *Tools in Fluvial Geomorphology*: 633–660.

Koster EA, Castel II, Nap RL. 1993. Genesis and sedimentary structures of late Holocene aeolian drift sands in northwest Europe. *Geological Society, London, Special Publications* **72**: 247–267.

Kuenen PH. 1944. The Drentse riviertjes en het meander-vraagstuk: Overdruk uit Gedenkboek P. Tesch.

Langford RP. 1989. Fluvial-aeolian interactions: Part I, modern systems. *Sedimentology* **36**: 1023–1035. DOI:10.1111/j.1365-3091.1989.tb01540.x.

Langford RP, Chan MA. 1989. Fluvial-aeolian interactions. Part II, ancient systems. *Sedimentology* **36**: 1037–1051. DOI:10.1111/j.1365-3091.1989.tb01541.x.

Lapen D, Moorman B, Price J. 1996. Using ground-penetrating radar to delineate subsurface features along a wetland catena. *Soil Science Society of America Journal* **60**: 923–931.

Leopold LB, Wolman MG. 1960. River meanders. *Geological Society of America Bulletin* **71**: 769–793.

Lespez L, Viel V, Rollet A, Delahaye D. 2015. The anthropogenic nature of present-day low energy rivers in western France and implications for current restoration projects. *Geomorphology* **251**: 64–76.

Lobeck AK. 1939. *Geomorphology, an Introduction to the Study of Landscapes*. McGraw-Hill: New York.

Lowry CS, Fratta D, Anderson MP. 2009. Ground penetrating radar and spring formation in a groundwater dominated peat wetland. *Journal of Hydrology* **373**: 68–79.

Mactaggart B, Bauer J, Goldney D, Rawson A. 2008. Problems in naming and defining the swampy meadow – an Australian perspective. *Journal of Environmental Management* **87**: 461–473.

Madsen AT, Murray A, Andersen T, Pejrup M, Breuning-Madsen H. 2005. Optically stimulated luminescence dating of young estuarine sediments: a comparison with 210 Pb and 137 Cs dating. *Marine Geology* **214**: 251–268.

Makaske B. 2001. Anastomosing rivers: a review of their classification, origin and sedimentary products. *Earth-Science Reviews* **53**: 149–196.

Makaske B, Maas G. 2015. *Handboek Geomorfologisch Beekherstel*. Wageningen, Alterra.

Makaske B, Maas G, Grootjans A, Meijles E, Everts H, De Vries N. 2015. Veen verschijnt en verdwijnt - Grondwaterstromen en veenvorming, Landschapsbiografie van de Drentsche Aa. Assen, Koninklijke Van Gorcum, 54–81.

Makaske B, Smith DG, Berendsen HJ. 2002. Avulsions, channel evolution and floodplain sedimentation rates of the anastomosing upper Columbia River, British Columbia, Canada. *Sedimentology*. **49**: 1049–1071.

McMillan SK, Vidon PG. 2014. Taking the pulse of stream restoration practices: moving towards healthier streams. *Hydrological Processes* **28**: 398–400. DOI:10.1002/hyp.10092.

Meijles E. 2015. Waterafvoer in de 20ste eeuw, Landschapsbiografie van de Drentsche Aa: Assen, Koninklijke Van Gorcum, 54–81.

Micheli E, Kirchner J. 2002a. Effects of wet meadow riparian vegetation on streambank erosion. 1. Remote sensing measurements of streambank migration and erodibility. *Earth Surface Processes and Landforms* **27**: 627–639.

Micheli E, Kirchner J. 2002b. Effects of wet meadow riparian vegetation on streambank erosion. 2. Measurements of vegetated bank strength and consequences for failure mechanics. *Earth Surface Processes and Landforms* **27**: 687–697.

Mook W, Streurman H. 1983. Physical and chemical aspects of radiocarbon dating. Proceedings of the First International Symposium on 14C and Archaeology, Groningen, 1981, 31–55.

Nanson GC, Croke JC. 1992. A genetic classification of floodplains. *Geomorphology* **4**: 459–486. DOI:10.1016/0169-555X(92)90039-Q.

Nanson RA. 2009. The evolution of peat-swamp channels and organic floodplains, Barrington Tops, New South Wales, Australia. *Geographical Research* **47**: 434–448. DOI:10.1111/j.1745-5871.2009.00596.x.

Nanson RA. 2010. Flow fields in tightly curving meander bends of low width-depth ratio. *Earth Surface Processes and Landforms* **35**: 119–135.

Nanson RA, Cohen TJ. 2014. Headwater peatland channels in south-eastern Australia; the attainment of equilibrium. *Geomorphology* **212**: 72–83. DOI:10.1016/j.geomorph.2013.11.011.

Nanson RA, Nanson GC, Huang HQ. 2010. The hydraulic geometry of narrow and deep channels; evidence for flow optimisation and controlled peatland growth. *Geomorphology* **117**: 143–154. DOI:10.1016/j.geomorph.2009.11.021.

Neal A. 2004. Ground-penetrating radar and its use in sedimentology: principles, problems and progress. *Earth-Science Reviews* **66**: 261–330. DOI:10.1016/j.earscirev.2004.01.004.

Notebaert B, Verstraeten G. 2010. Sensitivity of West and Central European river systems to environmental changes during the Holocene: a review. *Earth-Science Reviews* **103**: 163–182. DOI:10.1016/j.earscirev.2010.09.009.

Page SE, Rieley J, Shotyk Ø, Weiss D. 1999. Interdependence of peat and vegetation in a tropical peat swamp forest. *Philosophical Transactions of the Royal Society of London B: Biological Sciences* **354**: 1885–1897.

Pîrnău RG, Mihu-Pintilie A, Bodi G, Asăndulesei A, Niac□u L. 2015. Ground penetrating radar as non-invasive method used in soil science and archaelogy. *Soil Forming Factors and Processes from the Temperate Zone* **13**: 15–32.

Prescott JR, Hutton JT. 1994. Cosmic ray contributions to dose rates for luminescence and ESR dating: large depths and long-term time variations. *Radiation Measurements* **23**: 497–500.

Preusser F, Degering D, Fuchs M, Hilgers A, Kadereit A, Klasen N, Krbetschek M, Richter D, Spencer JQ. 2008. Luminescence dating: basics, methods and applications. *Quaternary Science Journal* **57**: 95–149.

Prosser IP, Chappell J, Gillespie R. 1994. Holocene valley aggradation and gully erosion in headwater catchments, south-eastern highlands of Australia. *Earth Surface Processes and Landforms* **19**: 465–480. DOI:10.1002/esp.3290190507.

Proulx-McInnis S, St-Hilaire A, Rousseau AN, Jutras S. 2013. A review of ground-penetrating radar studies related to peatland stratigraphy with a case study on the determination of peat thickness in a northern boreal fen in Quebec, Canada. *Progress in Physical Geography* **37**: 767–786. DOI:10.1177/0309133313501106.

Rajchl M, Uličný D. 2005. Depositional record of an avulsive fluvial system controlled by peat compaction (Neogene, Most Basin, Czech Republic). *Sedimentology* **52**: 601–625. DOI:10.1111/j.1365-3091.2005.00691.x.

Reimer PJ, Baillie MG, Bard E, Bayliss A, Beck JW, Blackwell PG, Bronk RC, Buck CE, Burr GS, Edwards RL. 2009. IntCal09 and Marine09 radiocarbon age calibration curves, 0–50 000 years cal BP. *Radiocarbon* **51**: 1111–1150.

Reimer PJ, Bard E, Bayliss A, Beck JW, Blackwell PG, Bronk Ramsey C, Buck CE, Cheng H, Edwards RL, Friedrich M. 2013. IntCal13 and Marine13 radiocarbon age calibration curves 0-50,000 years cal BP **55**(4): 1869–1887.

Sear DA, Arnell NW. 2006. The application of palaeohydrology in river management. *Catena* **66**: 169–183. DOI:10.1016/j.catena.2005.11.009.

Sevink J, Koster EA, van Geel B, Wallinga J. 2013. Drift sands, lakes, and soils: the multiphase Holocene history of the Laarder Wasmeren area near Hilversum, the Netherlands. *Netherlands Journal of Geosciences* **9**: 243–266. DOI:10.1017/S0016774600000196.

Spek T, Elerie H, Bakker JP, Noordhoff I. 2015. Landschapsbiografie van de Drentsche Aa: Assen, Koninklijke Van Gorcum.

Stenberg L, Tuukkanen T, Finér L, Marttila H, Piirainen S, Kløve B, Koivusalo H. 2015. Evaluation of erosion and surface roughness in peatland forest ditches using pin meter measurements and terrestrial laser scanning. *Earth Surface Processes and Landforms*: 1299–1311. DOI:10.1002/esp.3897.

Thorndycraft VR. 2013. *Palaeohydrology, In Encyclopedia of Quaternary Science* (2nd edn). Elsevier, Amsterdam, 253–258. doi: 10.1016/B978-0-444-53643-3.00114-X

Thorne C. 1982. Processes and mechanisms of river bank erosion. *Gravel-Bed Rivers* 227–259.

TNO. 2015. DINOLoket. *Utrecht*.

Törnqvist T, de Jong AF, Oosterbaan WA, Van der Borg K. 1992. Accurate dating of organic deposits by AMS 14C measurement of macrofossils. *Radiocarbon* **34**: 566–577.

Van Balen R, Kasse C, De Moor J. 2008. Impact of groundwater flow on meandering; example from the Geul River, The Netherlands. *Earth Surface Processes and Landforms* **33**: 2010–2028.

Van der Meene E, Van der Staay J, Teoh LH. 1979. The Van der Staay suction-corer: a simple apparatus for drilling in sand below groundwater table, Rijks Geologische Dienst.

Van den Berg M, Beets D. 1987. Saalian glacial deposits and morphology in The Netherlands. In *Tills and Glaciotectonics*. Balkema: Rotterdam; 235–251.

Van der Plicht J. 2005. WinCal25. Groningen, the Netherlands: Center for Isotope Research, University of Groningen.

Van Heerd R, Van't Zand R. 1999. Productspecificatie Actueel Hoogtebestand Nederland: Rijkswaterstaat Meetkundige Dienst, Delft.

Van Overmeeren RA, Sariowan SV, Gehrels JC. 1997. Ground penetrating radar for determining volumetric soil water content; results of comparative measurements at two test sites. *Journal of Hydrology* **197**: 316–338. DOI:10.1016/S0022-1694(96)03244-1.

Vermeulen B, Hoitink A, Berkum S, Hidayat H. 2014. Sharp bends associated with deep scours in a tropical river: The river Mahakam (East Kalimantan, Indonesia). *Journal of Geophysical Research: Earth Surface* **119**: 1441–1454.

Wallinga J, Davids F, Dijkmans J. 2007. Luminescence dating of Netherlands' sediments. *Netherlands Journal of Geosciences – Geologie en Mijnbouw* **86**(3).

Wallinga J, van der Staay J. 1999. Sampling in water logged sands with a simple hand operated corer. *Ancient TL* **17**: 59–61.

Walter RC, Merritts DJ. 2008. Natural streams and the legacy of water-powered mills. *Science* **319**: 299–304. DOI:10.1126/science.1151716.

Wastiaux C, Halleux L, Schumacker R, Streel M, Jacqmotte JM. 2000. Development of the Hautes-Fagnes peat bogs (Belgium): new perspectives using ground-penetrating radar. In *Suo* (Vol. 51, No. 3, pp. 115-120). Suoseura-Finnish Peatland Society.

Watters JR, Stanley EH. 2007. Stream channels in peatlands: The role of biological processes in controlling channel form. *Geomorphology* **89**: 97–110. DOI:10.1016/j.geomorph.2006.07.015.

Wilde S, Tanzer C. 1965. De Alluviale Gronden van de Maas, de Roer, en de Geul in Limburg (Alluvial Soils of the Rivers Maas, Roer, and Geul). *Soil Science Society of America Journal* **29**: iv–iv.

Wintle AG, Murray AS. 2006. A review of quartz optically stimulated luminescence characteristics and their relevance in single-aliquot regeneration dating protocols. *Radiation Measurements* **41**: 369–391.

Wohl E, Angermeier PL, Bledsoe B, Kondolf GM, MacDonnell L, Merritt DM, Palmer MA, Poff NL, Tarboton D. 2005. River restoration. *Water Resources Research* **41**: W10301.

Supporting Information

Additional supporting information may be found in the online version of this article at the publisher's web site.